Earth's Future

RESEARCH ARTICLE
10.1029/2020EF001870

Rock Water as a Key Resource for Patchy Ecosystems on Shallow Soils: Digging Deep Tree Clumps Subsidize Surrounding Surficial Grass

Nicola Montaldo[1], Roberto Corona[1], Matteo Curreli[1], Serena Sirigu[1], Luca Piroddi[1], and Ram Oren[2,3]

[1]Dipartimento di Ingegneria Civile, Ambientale e Architettura, Università di Cagliari, Italy, [2]Nicholas School of the Environment and Pratt School of Engineering, Duke University, Durham, NC, USA, [3]Department of Forest Sciences, University of Helsinki, Finland

Supporting Information:
- Supporting Information S1

Correspondence to:
N. Montaldo and R. Oren, nmontaldo@unica.it; ramoren@duke.edu

Citation:
Montaldo, N., Corona, R., Curreli, M., Sirigu, S., Piroddi, L., & Oren, R. (2020). Rock water as a key resource for patchy ecosystems on shallow soils: Digging deep tree clumps subsidize surrounding surficial grass. *Earth's Future*, *8*, e2020EF001870. https://doi.org/10.1029/2020EF001870

Received 22 OCT 2020
Accepted 1 DEC 2020

Author Contributions
N. Montaldo and R. Oren designed the research and analyzed the data. M. Curreli, R. Corona, and S. Sirigu collected the data, and analyzed the data. R. Corona performed model simulation. L. Piroddi analyzed ERT measurements. N. Montaldo and R. Oren wrote the manuscript.

Abstract Mediterranean mountainous areas of shallow soil often display a mosaic of tree clumps surrounded by grass. The combined role and dynamics of water extracted from the underlying rock, and the competition between adjacent patches of trees and grass, has not been investigated. We quantified the role rock water plays in the seasonal dynamics of evapotranspiration (*ET*), over a patchy landscape in the context of current and past seasonal climate changes, and land-cover change strategies. Soil water budget suggests deep water uptake by roots of trees (0.8–0.9 mm/d), penetrating into the fractured basalt, subsidized grass transpiration in spring through hydraulic redistribution. However, in summer trees used all the rock water absorbed (0.79 mm/d). A 15-year data set shows that, with increasing seasonal drought-severity (potential *ET*/precipitation) to >1.04, the vertical water flux through the bottom of the thin soil layer transitions from drainage to uptake in support of *ET*. A hypothetical grass-covered landscape, with no access to deep water, would require 0.68–0.85 mm/d more than is available, forcing shortened growing season and/or reduced leaf area. Long-term decreasing winter precipitation and increasing spring potential *ET* suggest drying climate, so far with stable vegetation mosaic but progressively earlier peak of grass leaf area. Intervention policies to increase water yield by reducing tree cover will curtail grass access to rock moisture, while attempting to increase tree-related products (including carbon sequestration) by increasing forest cover will limit water availability per tree leaf area. Both changes may further reduce ecosystem stability.

Plain Language Summary In drier regions, individual trees or tree clumps are often surrounded by seasonal vegetation. Increasing climatic drought, form decreasing precipitation in winter and increasing potential evapotranspiration in spring, is common in these regions. Where the balance among vegetation types in a mosaic depends on deep water to subsidize transpiration, increasing drought may overwhelm the capacity for this subsidy, affecting both land cover and biosphere-atmosphere exchanges. Here we show that, in patchy ecosystems, nighttime hydraulic-lift of rock-moisture by wild-olive roots recharges the shallow soil, enough to support transpiration of grass and trees in spring, but only trees in summer. Thus, seasonal vegetation rely on the evergreen trees to maintain physiological activity in spring, while the evergreen trees rely on the inactivity of the seasonal component to maintain their own activity in the dry season. These ecosystems likely represent a spatiotemporal equilibrium of water supply, dynamically meeting the demand of two adjacent vegetation types of distinct seasonal phenology. The equilibrium is not only highly sensitive to climate change, but may be destabilized by policies aiming to increase carbon sequestration by increasing tree cover, or water yield by increasing seasonal vegetation cover, with additional consequences to decreasing tree survival or increasing surface temperature

1. Introduction

Dry regions are often characterized by heterogeneous ecosystems, where trees or tree clumps are competing for water with the surrounding grasses (Breshears, 2006; Detto et al., 2006; Montaldo et al., 2008; Sankaran et al., 2005; Scholes & Archer, 1997; Villegas et al., 2014). In these regions, climate change over the past century, manifested in trending meteorological regimes of decreasing precipitation and increasing

temperature, exacerbate tree-grass competition for water (Batisani & Yarnal, 2010; Brunetti et al., 2002; Caloiero et al., 2019; Ceballos et al., 2004; Garcia-Ruiz et al., 2011; Huang et al., 2016; Montaldo & Sarigu, 2017; Swain et al., 2016; Tabari et al., 2012). Tree cover in dry regions, and its spatial patterns, are variable, depending on water availability and incoming radiation (Sankaran et al., 2005), both reflecting topographic, climatic and edaphic factors, and ultimately producing the tree-grass mosaic on the landscape (Breshears, 2006; Moore et al., 2011; Villegas et al., 2014). In turn, the characteristics of the woody plant-grass mosaic influence the land-surface fluxes, having different seasonal dynamics in patches of tree canopy and adjacent intercanopy surface (Breshears, 2006; Montaldo et al., 2020). Evapotranspiration (*ET*) is the leading loss term in the water budget of semi-arid and arid regions (D. D. Baldocchi et al., 2004; Kurc & Small, 2004; Maselli et al., 2004; Reynolds et al., 2000; Rodriguez-Iturbe, 2000). Although *ET* estimates for these ecosystems are available, the sources of water and mechanisms for obtaining it, especially during dry periods, are often unclear (D. D. Baldocchi et al., 2004; Detto et al., 2006; Griebel et al., 2016; Kurc & Small, 2004). This is particularly so where tree clumps are growing on shallow soils surrounded by seasonal vegetation (Allen, 2009; Barbeta et al., 2015; Bornyasz et al., 2005; Lewis & Burgy, 1964).

There is increasing evidence suggesting that tree roots penetrating below thin soils through cracks, fractures and dissolution features, absorb and transpire sufficient amounts of water to sustain physiological activity in dry seasons (Breshears et al., 2009; Cannon, 1911; Eliades et al., 2018; McCole & Stern, 2007; Nie et al., 2017; Rempe & Dietrich, 2018; Schwinning, 2010; Yan et al., 2019), thus assuring survival. These roots allow trees to use, during the dry season, water infiltrating during wet seasons into fractured rocks, and held in soil pockets (Estrada-Medina et al., 2013; Rempe & Dietrich, 2018); indeed, root uptake of water stored in the underlying rock have been estimated to contribute 70%–90% of ET (Breshears et al., 2009; McCole & Stern, 2007; Schwinning, 2010). Remarkably, the contribution of water stored in the rocky strata to tree transpiration, and to ecosystem evapotranspiration, is commonly ignored in ecological and hydrological studies, and in modeling of biosphere-atmosphere exchanges (Rempe & Dietrich, 2018; Schwinning, 2010), prompting Schwinning (2010) to issue the challenge to elucidate the "eco-hydrology of roots in rocks."

The water balance of the surface soil layer can be described broadly as:

$$P - Q - ET - f_d = \Delta S \tag{1}$$

where P is precipitation, Q is runoff, ΔS is the variation of the water in the soil layer, and f_d is the vertical flux through the bottom of the soil layer from underlying substrate (i.e., positive when downward). While Q is typically a large loss term during the wet season, it is negligible during the dry season of semi-arid and arid regions (Corona et al., 2018; Montaldo & Sarigu, 2017). We expect drainage to dominate (positive) f_d during a typical wet season, but water uptake by roots in the rocky layer should dominate (negative) f_d during dry seasons. As climate aridity increases (Huang et al., 2016; Montaldo & Sarigu, 2017), the role of dry season f_d in the water balance may increase. This balance (Equation 1) has been often employed successfully in studies of *homogeneous* ecosystems (e.g., Imukova et al., 2016; Reichert et al., 2017; Scott, 2017).

Detto et al. (2006) and Montaldo et al. (2020) investigated a typical heterogeneous Mediterranean ecosystem located at Orroli in Sardinia (Italy; Montaldo et al., 2008, 2013), a patchy mixture of trees (mainly wild olive, *Olea europea var. sylvestris*) and grass growing on thin soil (~17 cm depth) above a fractured basalt. The latter study identified tree transpiration as the primary component of *ET* during the dry seasons – tree clumps maintained some summertime transpiration even though the thin soil was dry and its water content unchanging, suggesting access to subsoil water source. Indeed, the wild olive, a common Mediterranean species (Lumaret & Ouazzani, 2001; Terral et al., 2004), appear to tolerate well prolonged droughts (e.g., summer, 2003), increasingly common on the island (Montaldo & Oren, 2018; Montaldo & Sarigu, 2017). The species developed an adaptation strategy to increase reliance on a range of avoidance and tolerance mechanisms that maintain internal water status and metabolic activity during the dry periods (Connor et al., 2005; Fernandez et al., 1997; Lo Gullo & Salleo, 1998). This strategy consists of both control of transpiration rate, and water uptake by an extensive root system, which can penetrate the underlying fractured rocks. Subsoil water uptake is not unique to wild olive, demonstrated primarily, but not exclusively, in chaparral shrubs and several species of pines and oaks, growing mostly in regions with pronounced dry season and mountainous landscapes of shallow soils (Allen, 2009; Bornyasz et al., 2005; Breshears et al., 2009; Graham et al., 1997, 2010; Hubbert et al., 2001; Lewis & Burgy, 1964; McCole & Stern, 2007; Rose et al., 2003; Schwin-

ning, 2008; Sternberg et al., 1996; Witty et al., 2003; Zwieniecki & Newton, 1995), where roots do not reach the water table, but may extract water stored in the fractured bedrock (Witty et al., 2003).

In patchy landscapes, the partitioning of *ET* into its contributing components is a challenge, particularly during the dry season (Raz-Yasseef et al., 2010; Villegas et al., 2014). In such heterogeneous ecosystems, for example, tree clumps may reach for water extending roots not only into the rocky substrate below their canopies, but also horizontally into the soil and underlying rock of the surrounding areas covered with highly seasonal, shallow-rooted vegetation (Breshears, 2006; Breshears et al., 2009; House et al., 2003). It is thus unclear whether trees are competing with the grass for its limited accessible water, or facilitating grass transpiration and soil evaporation through hydraulic redistribution of rock moisture, such as often observed among the layers of deep soils (Dohn et al., 2013; Domec et al., 2010; Ludwig et al., 2004; Neumann & Cardon, 2012; Quijano et al., 2012). Although evapotranspiration from grass-covered patches can be high during the wet season, it decreases during the dry season to the low rate of evaporation from dry vegetation and bare soil. Nevertheless, this low rate of evaporation may account for an appreciable portion of dry season *ET*, and must be considered when searching for the source of water used by trees.

It is clear that the trees in this ecosystem must rely on water extraction from below the thin soil to support the transpiration of tree clumps (E_t) and *ET*, yet the amount of water supplied by the rocky substrate, its horizontal distribution, and how it is affected by seasonal precipitation and potential evaporation is not known. Also unknown is how these quantities are affected by droughts, of which frequency has been increasing (Caloiero et al., 2019; Montaldo & Sarigu, 2017; Swain et al., 2016). Moreover, the effect of increasing drought severity on the local water budget occurs on the background of past and, likely, future land cover change strategies (e.g., afforestation vs. deforestation). Tree cover varied in extent historically (Pungetti, 1985), showing an increase in woody vegetation over recent decades as traditional agro-silvopastoral activities in Mediterranean ecosystems declined (Chauchard et al., 2007; Falcucci et al., 2007; Poyatos et al., 2003; Puddu et al., 2012). More recently, tension has emerged between two ecosystem services, water yield and carbon-based products (e.g., wood and sequestered carbon) (Ovando et al., 2019). Policies aimed at maximizing water yield may be achieved by converting the mosaic to mostly seasonal vegetation, despite the consequences to increased erosion and surface temperature, and decrease in carbon storage, while policies aimed at maximizing carbon-based products as agricultural pressure decreases may compel conversion of pasture to forest, at the expense of water yield (Gentry & Lopez-Parodi, 1980; Guzha et al., 2018; Liski et al., 2003; Mohammad & Adam, 2010; Ovando et al., 2019). Regardless, policies reflected in land cover change strategies must conform to the climatic-edaphic capacity to support the desired vegetation mix, and how this capacity may change if drought severity continues to increase (Lindner et al., 2014; Stephens et al., 2010; Vilà-Cabrera et al., 2018).

We combined sap flux measured in trees across the eddy-covariance footprint with energy balance and eddy-covariance measurements to estimate *ET* and its components in this typical heterogeneous Mediterranean ecosystem (Montaldo et al., 2020). These measurements, together with measured precipitation and soil moisture, and modeled flux components, were combined into seasonal soil water balance, investigating the water sources supporting evapotranspiration, and testing the hypotheses: (**H1a**) Water taken up by tree roots from the rocky layer dominates *ET* and its components during dry seasons. We obtained limited qualitative information on horizontal distribution of wild olive roots, and soil moisture and water flow in such roots to evaluate the hypothesis (**H1b**) that rock moisture used by wild olive roots during the dry season is taken also from below the grass. Lastly, we hypothesized (**H2**) that trees compete with the grass, and thus reduce the amount of water evapo-transpired from the grass covered area. We analyzed these hypotheses in the context of past seasonal climate changes and potential land-cover change strategies.

2. Materials and Methods

2.1. Setting

Located on a gently sloping plateau in east-central Sardinia (39°41′12. 57”°N, 9°16′30. 34”°E, 500 m elevation, Orroli in the Sarcidano area), the site is covered by a patchy mixture of tree clumps with canopy cover of ∼33% of the footprint area (Figure S1), and interclump area displaying herbaceous and grass species during the wet season, transitioning to dry soil surface during the principally rainless summer. The dominating

wild olive in tree patches average ~4 m in height, with scattered emergent individuals of *Quercus suber* and shorter shrubs; vines often climb the trees.

The climate is maritime Mediterranean: mean annual precipitation (1922–2017) is 643 mm, with dry summers (averaging 11 mm in July); mean annual air temperature (T_a) is 14.6°C (mean T_a of 23.7°C in July). The silt loam soil (19% sand, 76% silt, 5% clay), has a bulk density of 1.38 g/cm^3 and a porosity of 53%; soil depth is ranging 0–50 cm, averaging 17 cm ± 6 cm (standard deviation, SD) above a fractured basalt. In the unusually dry May of 2017, manifested in earlier than normal senescence of grasses, electrical resistivity tomography (ERT), was used to detect singularities such as cracks, fractures and soil pockets in the rocks, and their relative water content (Muchingami et al., 2012; Nijland et al., 2010; Rodriguez-Robles et al., 2017; Travelletti et al., 2012). The 12 m long images (unit electrode spacing of 0.25 m) were collected along nine transects at 1 m intervals between two tree clumps. Rocks, cracks, soil pockets and water content were qualitatively estimated from the observed electrical resistivity map of each transect. Qualitative information on the horizontal extent of wild olive roots was based on two trenches. Each trench was 7 m long and 0.2 m wide, extending to the underlying rock; from 0.2 m long section of the trench, positioned at 1, 2, 3, 4, and 7 m distance from the tree clump, all tree roots were separated and dried at 75°C to a constant weight.

2.2. Soil and Micrometeorological Measurements

A 10 m tower was instrumented to measure land-atmosphere fluxes of energy and water from April 2003. The tower includes a Campbell Scientific CSAT-3 sonic anemometer and a Licor-7500 CO2/H2O infrared gas analyzer at 10 m above ground to measure velocity, temperature and gas concentrations at 10 Hz for the estimation of latent heat, and sensible heat fluxes through standard eddy-correlation methods (e.g., D. Baldocchi, 2003). Half hourly statistics were computed and recorded with a 23X data logger (Campbell Scientific Inc., Logan, Utah). The effect of the gentle slope of the plateau was removed by an axis rotation (Detto et al., 2006) and the Webb-Pearman-Leuning adjustment (Webb et al., 1980) was applied. Skin temperature of the tree canopy and grass/bare soil patches (using IRTS-P by Apogee Instrument), incoming and outgoing shortwave and longwave radiation to derive net radiation (using CNR-1 by Kipp & Zonen), and soil heat flux and temperature (using HFT3 REBS) at two locations close to the eddy-covariance tower, combined to generate the energy budget, were monitored and half-hourly means were recorded. T_a and relative humidity (*RH*) were measured at the tower to calculate vapor pressure deficit, further processed into day-length normalized daily mean (D_z; Oren et al., 1996). Precipitation (*P*) was measured using a PMB2 CAE rain gauge. Complete details on these measurements and data processing are available at Detto et al. (2006) and Montaldo et al. (2020).

Seven frequency domain reflectometer probes (FDR, Campbell Scientific Model CS-616) were inserted in the soil close to the tower (3.3–5.5 m away) to estimate moisture (θ) at half-hourly intervals in the thin soil layer, from April 2003. FDR calibration is described in Montaldo et al. (2020). During the summer of 2018, five dielectric water potential sensors (MPS-2; Decagon Devices, Inc.) were installed at 10 cm depth to monitor soil water potential (Ψ_s), one under the canopy and four in a grass covered area, using the same logging procedure.

The components of *ET* budget were evaluated for closure against eddy-covariance *ET* using the two-dimensional footprint model of Detto et al. (2006) for upscaling the components to the eddy-correlation contributing land-cover area. The approach uses the fractions of tree cover, grass cover, and bare soil in the flux footprint, which was obtained from a multispectral high spatial resolution (resolution of 2.8 m) satellite image (DigitalGlobe Inc.), based on a supervised classification scheme (Montaldo et al., 2008). Further details on upscaling component flux to the footprint area can be found in Detto et al. (2006) and Montaldo et al. (2008, 2020). We have also estimated the normalized difference vegetation index (NDVI) over the field site using Landsat satellite images (30 m spatial resolution), which were available from 1984 (temporal resolution of 16 days).

For an historical meteorological analysis, daily precipitations from 1922 were available from two nearby rain-gauge stations, Nurri and Villanova Tulo (located <10 km from the eddy-covariance tower, always in the Sarcidano area). We considered mean precipitations of the two stations, which are correlated with *P* at the Orroli station during the overlapping period of operation (correlation coefficient 0.90, $p < 0.001$; slope

of 1.08 and intercept of 0.41 mm/d of the linear interpolation with Orroli P). Daily air temperatures from 1922 were also available from another nearby station, Mandas (~12 km from the eddy-covariance station; correlation coefficient of 0.97, $p < 0.01$, slope of 0.91 and intercept of 2.24°C of the linear interpolation with Orroli T_a).

2.3. Sap Flow Measurements and Scaling

Sap flux in stems (J_s) was monitored from August 22, 2014 to July 9, 2017 using Granier-type heat dissipation sensors inserted in 11 stems, keeping the original configuration and signal processing (Granier, 1987). The stems were positioned in eight clumps in the eddy-covariance footprint, and scaled to represent transpiration per unit ground area of the clumps (after Oishi et al., 2008) based on diameter measurements of 1,615 stems in 21 clumps, and allometric relationship between stem diameter and sapwood area developed for the site. In each clump, we estimated the ratio A_{sw}/A_g (A_{sw} is the tree sapwood area, and A_g is the ground area of the clump's canopy projection), and scaled J_s to total tree transpiration within the clump area, E_t^{SF}, multiplying by with A_{sw}/A_g (Oren et al., 1998). Because we did not calibrate the sensors for the species and conditions, we verified the scaled fluxes comparing with estimate from the energy balance method (Detto et al., 2006), based mainly on canopy surface temperature (T_s), wind velocity, air temperature and radiometer measurements. Upscaling the sap-flux measurements to the eddy-covariance footprint scale ($E_{t,fp}$) was accomplished by multiplying E_t^{SF} by the fraction of tree canopy cover ($F_{fp,t}$, estimated using Equation 4 of Detto et al. [2006]). Due to missing data, we patched together portions of the time series from 2014 to 2016, capturing typical seasonal dynamics of sap-flux in a relatively dry year, beginning in spring (March 20) and ending in fall (November 19). We also used the data from the even drier spring of 2017 (for details see Montaldo et al., 2020).

In the summer of 2018, we installed the same type of sensor in two positions along one shallow root of sufficient diameter (~7 cm near the stem), one close to the stem, and one 3 m away in an area covered by dry grass for estimating root sap flow (J_r) (Domec et al., 2010). We further installed a modified thermal dissipation sensor (designed to monitor only the direction of flow, proximal, toward tree clumps, or distal, away from clumps; Domec et al., 2010) in one position of two roots under canopy, about 1 m from a stem, and four roots farther under the grass. These measurements were designed to help evaluate, qualitatively, the behavior of roots and water flow between the grass covered and tree covered areas, during a period in which the grass canopy already senesced yet low summer precipitation increased soil moisture under both cover types.

2.4. Soil Water Balance

We used Equation 1 for the seasonal soil water balance. From observed P, the surface runoff Q was estimated using the commonly used Soil Conservation Service (SCS) method (Chow, 1988; Ponce, 1989; Soil Conservation Service, 1972, 1986). We estimated the key parameter of the SCS method, the CN curve number, using the results of the rainfall simulator-based experiments of Wilson et al. (2014) for plot-scale runoff simulation, conducted at the site in 2010. For simulating the observed runoff coefficients of 0.8 (with rainfall intensity of 61.6 mm/h and wet antecedent moisture conditions (AMC), Wilson et al., 2014), a CN value of 89 (for AMC II; Ponce, 1989) was estimated.

Eddy-covariance observations were used for estimating ET, and θ observations for estimating the variation of the water in the soil layer ($\Delta S = \Delta\theta\ (1 - rc)\ d_s$, with d_s soil depth equal to 0.17 m, and rc rock content equals to 10%). f_d was estimated as residual term of Equation 1.

We estimated bare soil evaporation (E_{bs}) and grass transpiration (E_g) based on the observed soil moisture (θ) using a simple approach (verified in Montaldo et al., 2008): $E_{bs} = \alpha\ PE$, and $E_g = \beta_g PE$ [with $\alpha = -9.815\theta^3 + 9.173\theta^2 - 0.082\theta$ (Parlange et al., 1999), and $\beta_g = (\theta - 0.08)/(\theta_{lim,g} - 0.08)$, if $\theta \le \theta_{lim,g}$ and $\beta_g = 1$ if $\theta > \theta_{lim,g}$, where $\theta_{lim,g}$ is the grass limiting soil moisture (Montaldo et al., 2008)]. E_w was set to the rainfall interception, with storage capacity of 0.2 LAI (Noilhan & Planton, 1989), where LAI is the leaf area index. LAI was estimated for both grass and tree canopy separately using the land surface–vegetation dynamic model of Montaldo et al. (2008), calibrated for Orroli. Potential evapotranspiration (PE) was estimated based on the Thornthwaite equation (Thornthwaite, 1948), controlled by air temperature observations only.

Based on the above, we estimated the water budget terms of Equation 1 for each season of the 2014–2016 observation period and for the driest 2017 spring for which observed sap flow measurements were available. For each season, we estimated the pasture evapotranspiration contribution ($E_p = E_{bs,fp} + E_{g,fp}$), while $E_{t,fp}$ was based on scaled sap flux (and, at the end of fall, using the energy balance approach; Montaldo et al., 2020).

Assuming that upward f_d relies on uptake of water from the rocky layer by tree roots, and its discharge into the overlaying thin soil layer as a hydraulic redistribution (Domec et al., 2010; Neumann & Cardon, 2012), we reevaluated the fluxes under a hypothetical scenario in which the pasture grass cover the entire area, thus having no access to rock moisture, scaling E_{bs}, E_g (using $F_{fp,bs}$ and $F_{fp,g}$ respectively) and E_w (using $F_{fp,g}$ only) to represent pasture conditions over the entire area.

2.5. Modeling the Soil Water Balance and the Consequences of Prescribed Changes in the Fractions of Land Cover

A simplified model of land surface interactions was developed to predict soil water balance and allow evaluation of the effect of land cover change on *ET* and its components, and on water yield. The model simulates at daily scale the soil water balance of two layers, the surface soil layer and an active fractured rock layer with tree roots:

$$d_s \frac{\partial \theta_s}{\partial t} = P - Q - E_w - F_{fp,bs}E_{bs} - F_{fp,g}E_g - \xi_t F_{fp,t}E_{t,s} + f_d - D_r \quad (2)$$

$$d_r \frac{\partial \theta_r}{\partial t} = -\left(1 - \xi_t\right)F_{fp,t}E_{t,r} - f_d + D_r - L_e \quad (3)$$

where θ_s is the predicted soil moisture, θ_r is the predicted rock moisture, $E_{t,s}$ is the tree transpiration from the surface soil layer, $E_{t,r}$ is the tree transpiration from the fractured rock layer (with $E_t = \xi_t E_{t,s} + (1 - \xi_t) E_{t,r}$), d_r is the depth of the active fractured rock layer (=1.5 m), ξ_t is the percentage of tree root water uptake from the surface soil layer, f_d equals 3.3×10^{-9} $(\Psi_r - \Psi_s)/d_r$ [in m/s, Lee et al., 2005, where Ψ_r and Ψ_s are the soil water potential in the fractured rock layer and in the surface soil layer, respectively, and are related to soil moisture, following Clapp & Hornberger, 1978, through $\Psi_r = 0.01\ (\theta_r/0.4)^{3.5}$ and $\Psi_s = 0.7\ (\theta_s/0.5)^8$ in m]. D_r is the drainage (estimated using the unit gradient assumption of gravity drainage from the root zone, so that $D_r = k_{sat}$ $(\theta_s/0.5)^{17}$, where k_{sat} is the saturated hydraulic conductivity, following Clapp & Hornberger, 1978), L_e is the leakage, equals $k_{sat}\ (\theta_r/0.5)^{19}$ (again using the unit gradient assumption of gravity drainage), and $F_{fp,g}$, and $F_{fp,bs}$ are the fractions of grass cover and bare soil in the flux footprint, respectively (estimated using Equation 4 of Detto et al. [2006]), and $F_{fp,t} + F_{fp,g} + F_{fp,bs} = 1$. We estimated E_{bs} and E_g, using the same approach previously described (see Section 2.4) but with predicted soil moisture (θ_s) instead of observed soil moisture (θ). $E_{t,s}$, and $E_{t,r}$ are also predicted based on soil moisture using a simple approach: $E_{t,s} = \beta_{ts}\ PE$ [where $\beta_{ts} = (\theta_s - 0.06)/(\theta_{lim,\,s} - 0.06)$, if $\theta_s \le \theta_{lim,s}$, and $\beta_{ts} = 1.0$ if $\theta_s > \theta_{lim,s}$, and $\theta_{lim,s}$ is the limiting soil moisture for trees with roots in the surface soil layer], and $E_{t,r} = \rho_r \beta_{tr} PE$ [where $\beta_{tr} = (\theta_r - 0.2)/(\theta_{lim,r} - 0.2)$, if $\theta_r \le \theta_{lim,r}$, and $\beta_{tr} = 1.0$ if $\theta_r > \theta_{lim,r}$ with $\theta_{lim,r}$ the limiting soil moisture for trees with roots in the active fractured rock layer, and ρ_r, an index of the root resistance to water uptake from the rock is 0.6]. Hence, the ecosystem evapotranspiration is:

$$ET = F_{fp,t}E_t + F_{fp,g}E_g + F_{fp,bs}E_{bs} + E_w \quad (4)$$

We generated several land cover change scenarios ranging from a scenario of 100% pasture cover to one of 100% tree cover, changing $F_{fp,t}$ (=0, 0.1, 0.2, 0.4, 0.5, 0.6, 0.7, 0.8, 0.9, and 1) and *CN* (=96.4, 94.2, 91.9, 87.5, 85.2, 82.9, 80.7, 78.5, 76.2, and 74, respectively).

Analyzing the potential impact of land cover change strategies, we used the model to estimate *ET* for a 100% grass land-cover scenario over the 2003–2017 period for which eddy-covariance data are available for the actual ecosystem, and tree transpiration for the opposite scenario of 100% tree cover over a dry year, and compare these estimates with those for the actual ecosystem. Furthermore, we evaluated the soil water balance components for the historical 1922–2017 period over the complete range of possible $F_{fp,t}$ (from 0 to 1).

Because the soil water balance model is sensitive to soil and vegetation parameters (Franks et al., 1997; Montaldo et al., 2003), we evaluated the effect of these uncertainties in our analysis, using a global multivariate approach (Franks et al., 1997; Montaldo et al., 2003) based on a Monte Carlo simulation framework, prescribing uncertainty in four key model parameters: the saturated hydraulic conductivity, and the three limiting soil moisture values in the beta functions of grass and tree transpiration estimates.

2.6. Statistical Data Analysis

Observed data at the Orroli station were analyzed at monthly and seasonal time scales, using typical statistical index (mean, μ, and standard deviation, SD).

Trends of *P, PE* and the soil water balance terms were computed using the Mann-Kendall nonparametric test (Hensel & Hirsch, 2002; Kendall, 1938; Sneyers, 1990). The Mann-Kendall τ measures the monotonic relationship between two variables, and it is less sensitive to outliers and missing data values. The Theil-Sen slope method was used to estimate the slope linear trends (Sen, 1968; Theil, 1950). Generally, this estimator is frequently applied in climatology and for the analysis of the hydrometeorological time series (Amirabadizadeh et al., 2014; Hirsch et al., 1982; Hu et al., 2012; Mohsin & Gough, 2010) to define the rate of change, β. The Theil-Sen method and the Mann-Kendall test are strongly connected, with the β slope estimator related to the Mann-Kendall τ test statistic (Montaldo & Sarigu, 2017).

Finally, the common standard precipitation index (SPI) has been used for identifying droughts in the precipitation time series both at seasonal and annual time scales (Guttman, 1998; Mishra & Singh, 2009). First a probability density function (a gamma distribution) that describes the long-term time series of rainfall observations was estimated, then the cumulative probability of an observed precipitation amount was computed. The inverse normal (Gaussian) function, with mean zero and variance one, was then applied to the cumulative probability distribution function, which results in SPI. We have classified droughts as severe droughts for SPI < -1.0, and extreme droughts for SPI < -2.0 (Livada & Assimakopoulos, 2007; Mishra & Singh, 2009).

3. Results

Dynamics of monthly soil moisture was almost in phase with precipitation over the 2003–2017 period (Figure 1a), but reached highest values in January and February, later then the wettest months (November and December), reflecting the combination of high *P* and low *ET*. Despite spring *P*, soil moisture decreased with increasing ET_{EC} (Figure 1b), peaking in May due to favorable conditions. In contrast to the large absolute variability of *ET*, tree transpiration was less variable during the 2014–2016 observation period, reaching highest rates in July and lowest in October. While predicted E_w was almost negligible all year, grass transpiration was high in spring, reaching highest rates in May, and diminishing thereafter as the grass senesced in summer (Figure 1c). Consequently, in summer, predicted bare soil evaporation exceeded grass transpiration, reaching highest rates in July (Figure 1c).

3.1. Water Balance and the Source of Evapotranspiration

The estimated water balance terms for spring, summer and fall of the 2014–2016 observation period and for the driest 2017 spring are in Figure 2. Evapotranspiration, as the sum of its components, $E_p + E_{t,fp} + E_w$, agreed without bias with estimates based on the eddy-covariance method, ET_{EC}, with differences (of +1.6% and 2.2%) only in the summer and fall (Figure 2). As expected, surface runoff occurred only in fall, when rainfall increased sufficiently to produce *Q* averaging ~0.14 mm/d, or 9.8% of *P*; due to both low *P* and high evaporative demand, *Q* was negligible during spring and summer. In both springs and summer, f_d was negative, meaning trees were absorbing water from the rocky substratum. In contrast, owing to low *ET* in fall, which in 2014 was not particularly rainy, the flux through the bottom of the thin soil layer was downward as drainage, recharging deeper reservoirs. As a check, we estimated the gravitational drainage in the three seasons using θ and the Clapp and Hornberger (1978) relationship [$k = 5 \times 10^{-6}\,(\theta/0.5)^{19}$; Montaldo

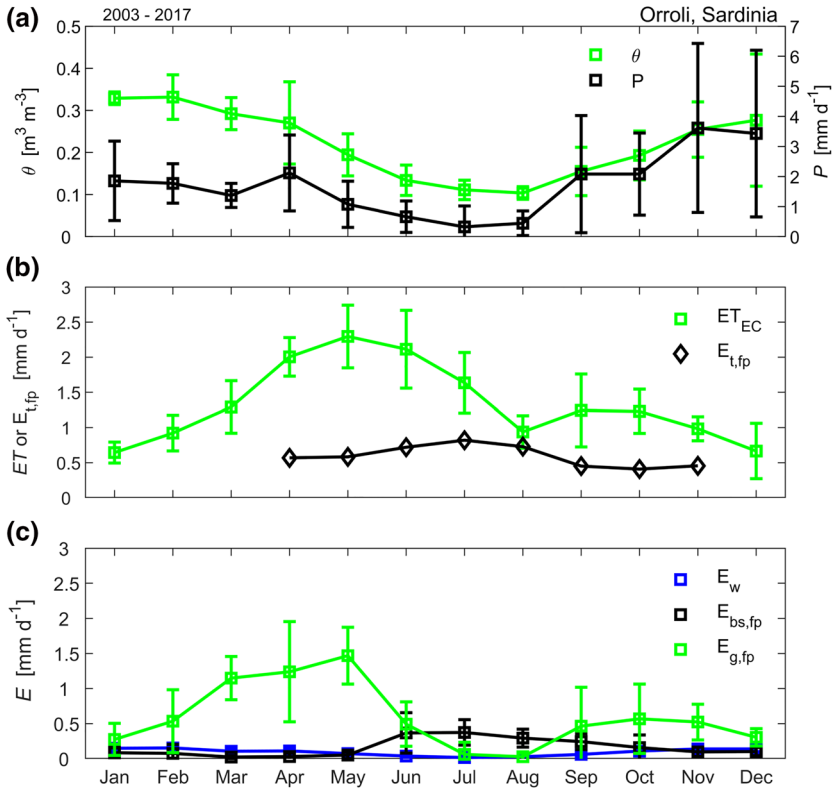

Figure 1. Monthly means (and standard deviations; $n = 10$ years except for tree transpiration) of: (a) observed precipitation (P) and soil moisture (θ); (b) observed ecosystem evapotranspiration (ET), and tree transpiration ($E_{t,fp}$; from the 2014–2016); (c) modeled wet-surface evaporation (E_w), bare soil evaporation ($E_{bs,fp}$), and grass transpiration ($E_{g,fp}$). All flux values scaled to the entire landscape.

et al., 2008]. Drainage was negligible in spring and summer (<0.01 mm/d), reaching 0.06 mm/d in fall, equal to the budget-based estimate of $f_d = 0.06$ mm/d (Figure 2c).

The budget-based approach produced an estimate of root water uptake from the rocky substratum of 62% of ET in summer, 45% of ET in the wetter spring of 2016, but reaching 64% of ET in the dry 2017 spring. Mean seasonal $E_{t,fp}$ was lowest in fall (0.43 mm/d) and highest in summer (0.74 mm/d). Spring ET during the wetter 2016 (1.84 mm/d) was double that of the fall (0.90 mm/d). The seasonal change of soil water content (considering the entire season) was negligible in summer, negative in spring and positive in fall.

In spring and summer, fluxes were also reevaluated under a hypothetical scenario in which the pasture grass cover the entire area (Figures 2d and 2e), and therefore the source of water from rock moisture was not available. Scaling E_{bs}, E_g, and E_w suggests that, depending on the spring, a daily deficit of ~0.70 or 0.86 mm/d will occur (Figure 2d), meaning the grass will not be able to sustain its current activity. In summer, with lower grass cover activity, and the soil dry, the daily deficit will be less (~0.28 mm/d, Figure 2e), suggesting that water taken up by trees from the rocky stratum (Figure 2b) is mainly for their own use. Without the tree component, ET in summer is reduced by 40%.

Qualitative information confirmed that rock moisture used by wild olive roots during the spring and summer was taken also from below the grass. From the two soil trenches we derived information on horizontal distribution of wild olive root density (Figure 3). For both trenches, root density was highest near the edge of clumps (9.3 kg/m^3 and 16.5 kg/m^3), showing a similar relative decrease with distance from the edge (Dt). The normalized root densities (NRD, normalized to 1.0 at 1 m from the edge) decreased such that $NRD = 0.897Dt^{1.302} + 0.107$ ($R^2 = 0.98$, $p < 0.01$; Figure 3a). At 7 m from the clumps, about halfway to the next clump in the direction of the trench, roots density seemed to stabilize at ~20% of the density at 1 m. While digging trenches to determine root distribution, second-order tree

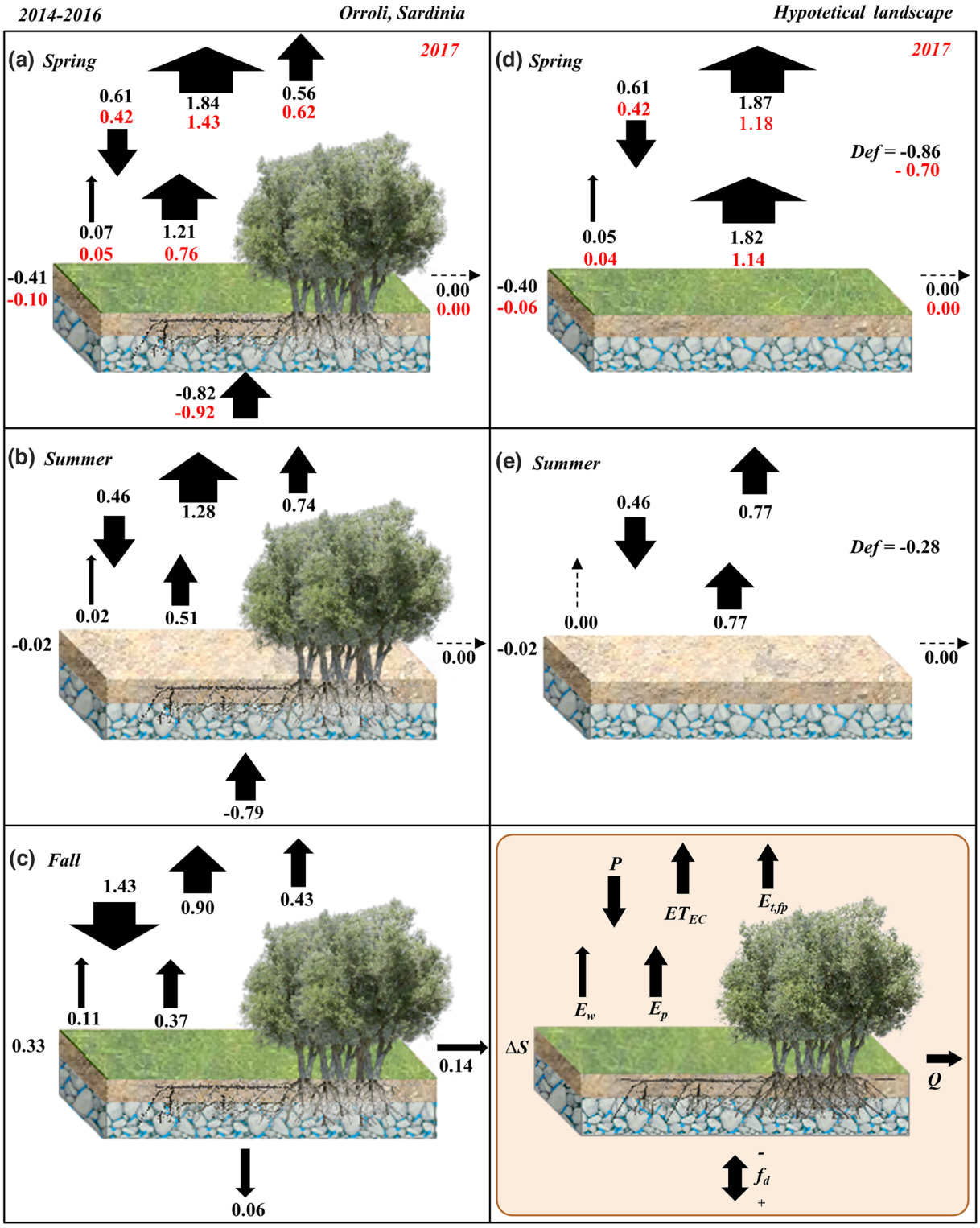

Figure 2. Soil water balance at the Orroli site with trees, and grass or bare soil in (a) spring, (b) summer and (c) fall, and of a hypothetical site with grass or bare soil only in (d) spring, and (e) summer. P: precipitation; ΔS: changes of soil water content; f_d: vertical flux through the bottom of the soil layer; ET: evapotranspiration; $E_{t,fp}$: transpiration from scaled sap flux normalized to the footprint area; E_p: footprint-scaled pasture evapotranspiration (=bare soil evaporation + grass transpiration); E_w: footprint-scaled wet evaporation; Q: surface runoff; Def: the closure term of the soil water balance (deficit). All the components of the soil water balance are mean seasonal quantities expressed in mm/d. Black text represents 2014–2016, and red text represents 2017.

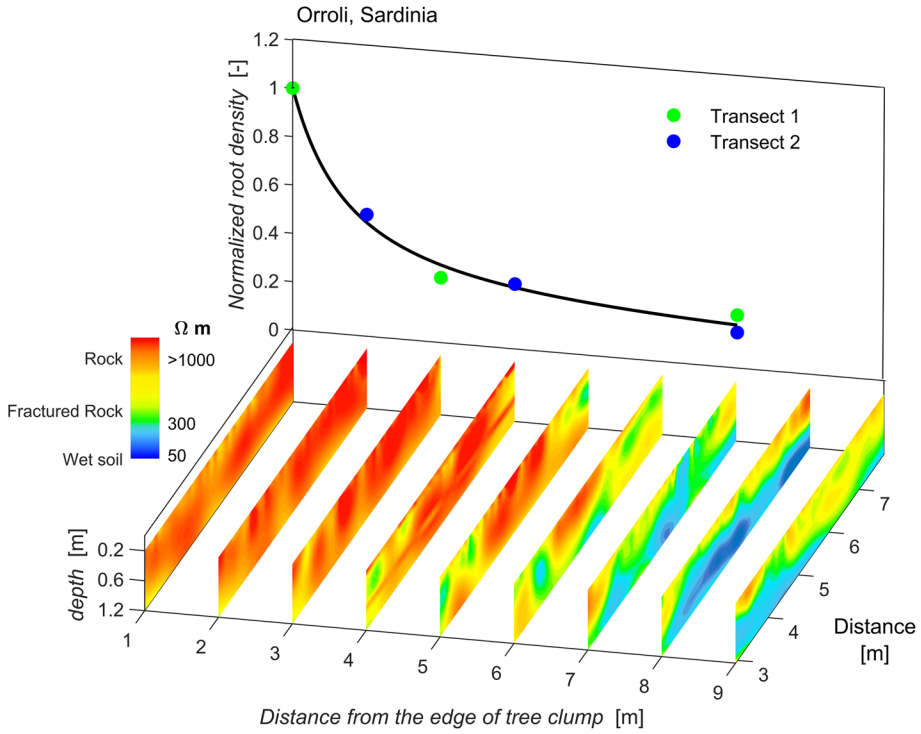

Figure 3. (a) Normalized density of transport roots along 7 m transect from the edge of two tree clumps. (b) inverse model electrical resistivity (in Ohm m) tomography (ERT) images, indicating rock fractures and soil pockets in the subsurface layer (0.2–1.2 m) in transects perpendicular to a root trench at 1 m intervals from the edge of a tree clump.

roots branching from the horizontal first order roots and penetrating vertically into the fractured basalt were observed. From the ERT information along the transects, we note that fractures, cracks and soil pockets were randomly distributed in the basalt, vertically and horizontally distributed, and surface moisture was higher in the rock fractures moving away from the tree clumps (Figure 3b). A thick rocky layer dominated the ground near the clump, but was not apparent near the surface with increasing distance (Figure 3b).

Using the soil water potential and root sap flow measurements during July 2018, we evaluated qualitatively the horizontal water flux between the area under the canopy and in the pasture, in the surface soil layer, and how it is supported by roots in the fractured rocks (Figure 4). July 2018 was a dry month following an unusually wet June, during which the soil saturated. Hence, ψ_s decreased from saturated to dry conditions both under the clump canopy and in the pasture, but at clearly different rates (Figure 4a). Under the canopy, water content decreased quickly due to tree water uptake; in the open, the senesced grass not only did not transpire, but may have slowed down evaporation; thus, a soil water potential gradient developed between the pasture area and tree clumps (Figure 4a; ψ_s gradient was significantly different from 0.0 during the period represented by the horizontal bar; one sample t-test $p < 0.05$). This is consistent with the directional flow measurements, showing persistent proximal flow during both day and night from roots in the pasture (Figure 4b). Roots near the clumps showed proximal flow only in daytime, but distal flow at nighttime, likely from rock moisture recharging the overlaying soil near the clumps (Figure 4b and left panel of Figure 4d). Then, as the gradient decreased later in the month (Figure 4a), nighttime flow ceased, and unchanging soil moisture suggest that root-soil contact in the dry soil decreased and the proximal flow observed during most of the daytime hours in roots near and far from the clumps (Figure 4b), was supplied by rock moisture uptake (right panel of Figure 4d). Sap flux of roots near clumps was low relative to that in stems, but nearly invariable (Figure 4c), while that of distant roots was similar to the stem sap flux, but decreased in relative terms as the soil dried; this suggests that when the shallow soil dries, limits to water uptake are imposed by access to rock moisture only (Figure 4d).

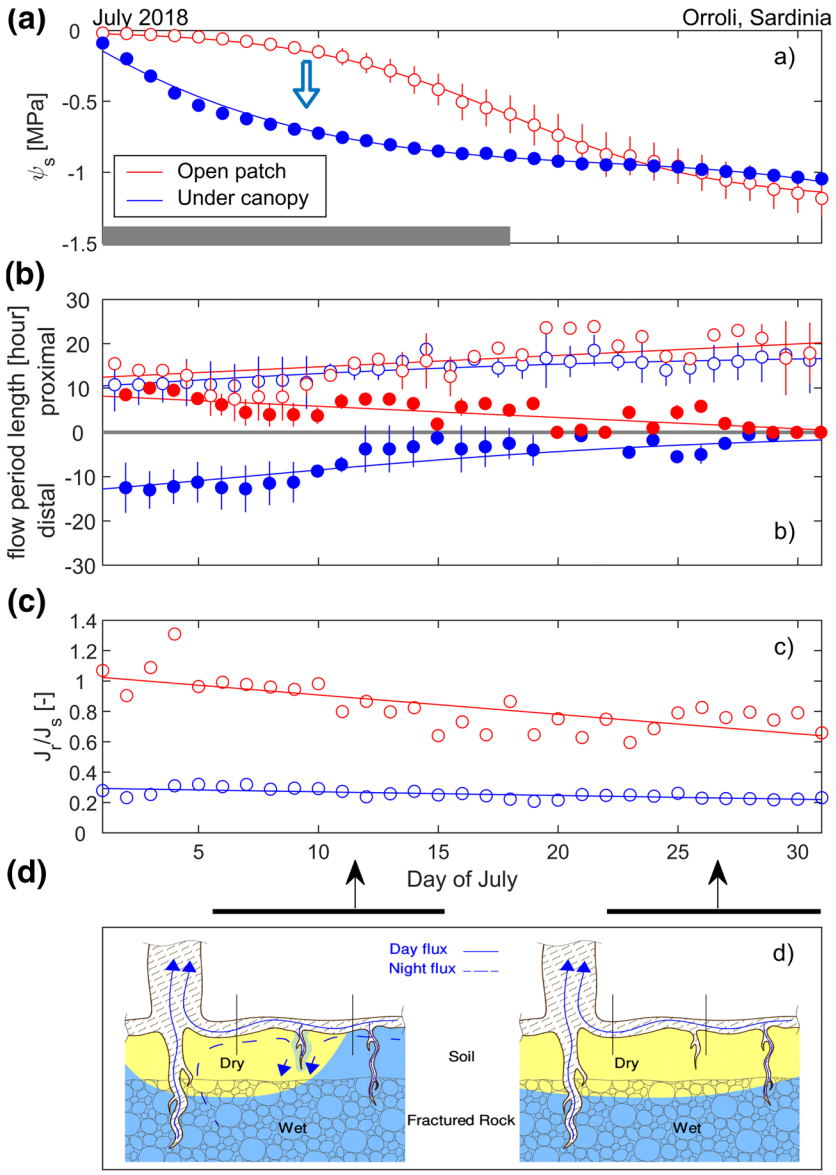

Figure 4. Over a drying cycle, (a) a comparison between soil water potential (ψ_s) of a probe under the canopy and the mean ($n = 4$, and standard deviations) of probes in the pasture area. The blue arrow indicates the direction of the force for water flow, and the horizontal gray line at the bottom indicates the days in which the two series are different ($p < 0.05$, one sample t-test). (b) The mean flow period length (in hours; proximal is toward the tree) of daytime (open points) and nighttime (filled points) of directional flow sensors under the canopy ($n = 2$) in the senesced grass-covered area ($n = 5$; mean and standard deviations). (c) The ratios of root sap flow (J_r), one measured near the stem and the other in the grass-covered area (3 m from a tree clump) to mean ($n = 6$) stem sap flow (J_s). (d) Schematic representation of diurnal and nocturnal sap flux between trees and grass-covered area as soil drying progressed from near the tree clump; blue area represents moist soil and fractured rock.

The key role in water uptake played by roots in the rocky substratum is highlighted when the seasonal contributions of f_d to ET is viewed in relation to the seasonal index of dryness (PE/P, e.g., Zhang et al., 2001) (Figure 5). For the analysis of the reliance of ET on f_d, we added available seasonal data collected at the Orroli flux tower since 2003 (10 springs and summers, 6 falls, 2 winters; note that data were not available for additional seasons). f_d was estimated as before as the residual term of the soil water balance (Equation 1), using measured P, ΔS, and ET (the latter observed at the eddy-covariance tower), and estimated Q [based on the Soil Conservation Service (1972; 1986) method]. In all winter and fall seasons, f_d/ET values were

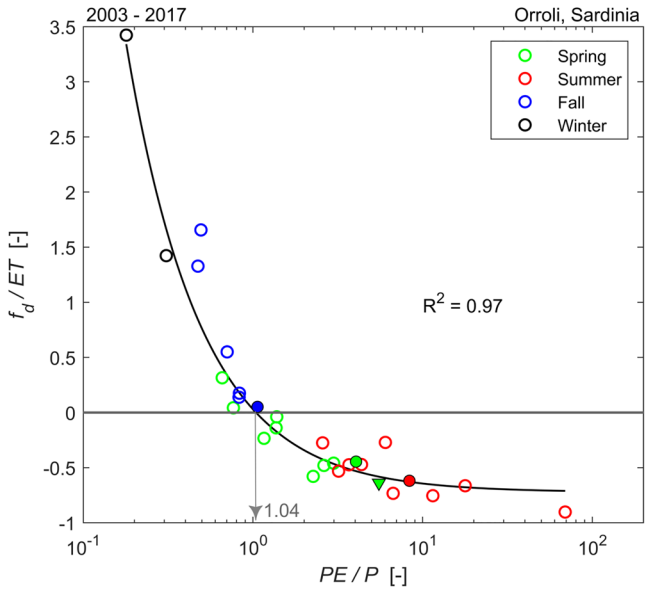

Figure 5. The contribution of the vertical flux through the bottom of the soil layer (f_d) to evapotranspiration (ET) versus the index of dryness (PE/P, potential evaporation/precipitation). Negative values indicate water taken up by wild olive roots from the underlying rocky substrate; positive values indicate drainage. Filled circles are for 2014–2016 time series, the filled triangle is for the spring 2017.

positive, and were highly variable, reflecting the variability of precipitation and the early fall hydration state of the soil. The f_d/ET values were nearly all negative in summer and spring. The seasonal f_d/ET related to that of PE/P ($f_d/ET = 0.79PE/P^{-0.96}-0.74$, $R^2 = 0.97$, $p = 0.001$), showing no flux at PE/P of ~1.04 (Figure 5), close to, but significantly higher than 1.0 ($p < 0.001$ based on one-sample t-test vs. 100 randomly generated values considering 2% uncertainty in P and 20% uncertainty in ET).

3.2. Past Seasonal Climate Changes and Land Cover Change Strategies

At annual time scale, the trend of SPI was negative, with a Mann Kendall τ of −0.20 ($p = 0.01$) and a slope of −0.01/y. The frequency of severe annual droughts increased with time, the number doubling during the last 30 years of record relative to the previous 30 years. Winter P is key for recharging rock reservoir; a significant negative trend of winter P (observed in nearby stations) was observed (τ of −0.19 with $p = 0.010$, β of −0.011 mm/d/y) with a decrease of mean daily P from 3.1 to 2.1 mm/d over the 95-year record (Figure 6.1). Spring is the season of grass activity, during which grass and trees compete for resources. Similar to summer and autumn P time series, analysis of P time series shows that there is no significant negative trend in spring (Table 1), yet dry springs, such as that of 2017, are becoming more common in the later decades of the 95-year period, with 11 spring seasons having lower P than the μ—SD after 1950, increasing in frequency after 1980 (Figure 6.2). In contrast, PE shows no significant trend in winter (Figure 6.5), but a significantly positive trend in spring, summer and autumn (Figure 6, Table 1). Consequently, the dryness index (PE/P) was positive in both winter (Figure 6, τ of 0.16 with $p = 0.03$, β of 0.001/y) and spring (Figure 6, τ of 0.16 with $p = 0.03$, β of 0.006/y), meaning that the both key hydrologic seasons are becoming drier.

Using the simplified model (Equations 2 and 3), we estimated the main soil water balance terms, ET, f_d, and D_r and their 95-year trends (Figure 6). Beforehand, the model was calibrated and evaluated against fluxes measured in the current ecosystem using data of the 2003–2017 observation period ($\theta_{lim,g} = 0.17$, $\theta_{lim,s} = 0.18$, $\theta_{lim,r} = 0.3$, $k_{sat} = 5 \times 10^{-7}$ m/s; $\xi_t = 0.80$ if $\theta_s \geq 0.22$, otherwise 0.20), with reasonable agreement with estimates of ET, $E_{t,fp}$, and f_d (root mean square error of 0.51 mm/d, 0.47 mm/d, 0.09 mm/d, and R^2 of 0.57, 0.91, and 0.87, respectively). While ET was almost constant in all seasons over the 95-year period, f_d increased significantly in spring and summer, and the drainage decreased significantly in winter and spring due to increasingly dry conditions (Figure 6 and Table 1).

Using the NDVI time series, we observed that maximum NDVI of trees was almost constant over the recent 35 years (0.6 ± 0.04 mean and SD), slightly higher than the maximum NDVI of grass (0.5 ± 0.41). The spring peak activity of grass shifted to progressively earlier date over the recent 35 years, at a rate of ~0.4 day/year, estimated using a linear interpolation between the yearly peak day of grass NDVI, D_{NDVI}, and the yn, the number of years beginning 1984 ($D_{NDVI} = -0.77yn + 125.84$; $R^2 = 0.22$, $p = 0.02$). The trend was unrelated to that of increasing early spring temperature ($p = 0.70$). The seasonal peak activity date of trees, also falling in spring, did not change over the 35 years ($p = 0.11$).

Analyzing the potential impact of land cover change strategies, we evaluated the role of rock water supply and its hydraulic redistribution for ET of two extreme land-cover scenarios (Figure 7). Using the seasonal soil water balance approach (as in Figures 2d and 2e), we compared the ET of the actual ecosystem with a hypothetical ecosystem made of 100% pasture cover, modeled without access to rock moisture through hydraulic lift by tree roots (HR; Figure 7a). We used the available seasonal data collected at the Orroli site since 2003, and compared ET for a large range of the dryness index (=PE/P). In general, for increasing PE/P, ET first increased, reaching a maximum value of ~2.5 mm/d for PE/P ~1.2, then decreased for increasing

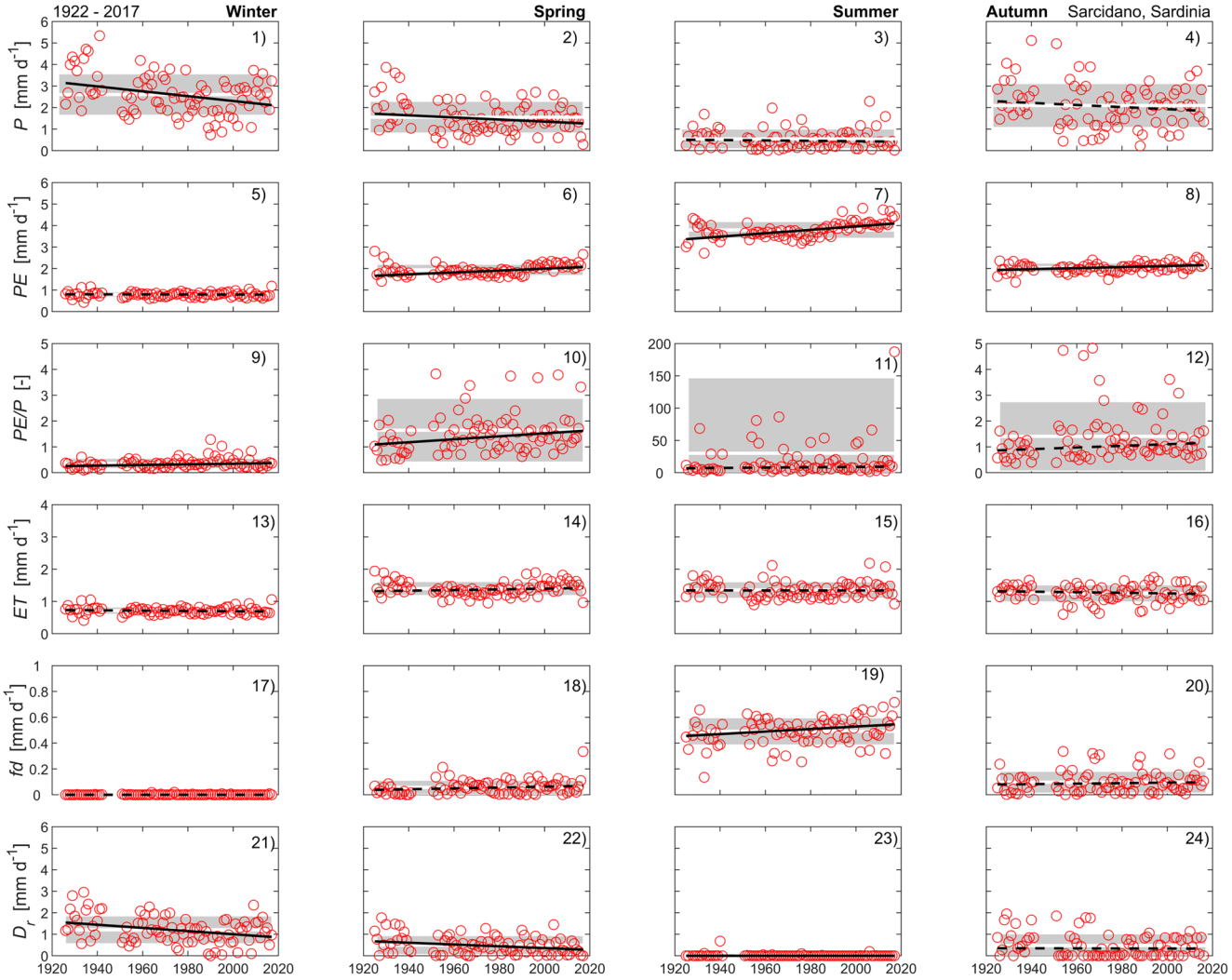

Figure 6. Historical seasonal, mean precipitation (P), potential evaporation (PE), index of dryness (PE/P) from two stations near Orroli in the area of Sarcidano, Sardinia, and predicted evapotranspiration (ET), vertical flux through the bottom of the soil layer (f_d), and drainage (D_r), represented by a white horizontal bar (mean) bracketed by gray bars (1 standard deviation). The trends using the Mann-Kendall approach are estimated with slopes from the Theil-Sen method (significant trends at $p < 0.01$, are continuous black lines, while not significant are dashed black lines).

drought. However, a grass-only landscape without access to tree-induced HR is predicted to have ET clearly dropping below that of the actual landscape as PE/P increased to >1. For the higher range of PE/P, ET of 100% pasture decrease to ~29% of the current ecosystem (Figure 7a).

The comparison between the fluxes from the actual landscape and the hypothetical 100% tree cover scenario focused on a dry year, using 2017 as example of a year characterized by a severe drought in spring and an extreme drought in summer (mean daily precipitation of 0.42 and 0.24 mm/d, SPI of −1.48 and −3.01 for spring and summer, respectively; Figure 7b). In this analysis, we are interested in how well trees will fare in the hypothetical ecosystem relative to current conditions, thus express tree transpiration per unit of leaf area, which relates to leaf conductance and photosynthetic rate if vapor pressure deficit is not responsive to the land-cover change. A landscape completely covered by trees only, leads to a decrease of tree transpiration per unit of leaf area ($E_{t,fp}/LAI$) in summer, with decreasing mean values of $E_{t,fp}/LAI$ down to 0.64 of the mean values of $E_{t,fp}/LAI$ for the actual case, and further to 0.54 at the end of the summer (Figure 7b). The increase of tree cover produced a faster depletion of water availability during the summer, leading to a persistently lower $E_{t,fp}/LAI$. Considering the whole 2003–2017 observation period, the mean summertime $E_{t,fp}/LAI$ of 100% tree cover case is predicted to be 0.8 of the actual case.

Table 1
Seasonal Mann Kendall τ Values (With p Value) and the Theil Sen Slopes (β) of the Trend Lines of Figure 6 of: Tree Transpiration at the Footprint Scale ($E_{t,fp}$); Grass Transpiration at the Footprint Scale ($E_{g,fp}$); Evapotranspiration (ET); Vertical Flux Through the Bottom of the Soil Layer (f_d); and Drainage (D_r)

	τ				p of τ				β [mm/d]			
	wi	sp	su	au	wi	sp	su	au	wi	sp	su	au
P	−0.191	−0.111	−0.046	−0.078	0.010	0.137	0.537	0.296	−0.011	−0.005	−0.001	−0.005
PE	−0.025	0.303	0.385	0.209	0.737	0.000	0.000	0.005	0.000	0.004	0.008	0.002
PE/P	0.157	0.158	0.074	0.105	0.035	0.034	0.322	0.105	0.001	0.006	0.026	0.003
ET	−0.076	0.079	0.037	−0.050	0.306	0.288	0.620	0.509	0.000	0.001	0.001	−0.001
f_d	0.077	0.151	0.171	0.059	0.302	0.043	0.022	0.432	0.000	0.000	0.001	0.000
D_r	−0.183	−0.184	−0.115	−0.094	0.014	0.013	0.123	0.208	−0.007	−0.004	0.000	0.000

Note. The 95-year long time series (1922–2017) is from the ecosystem at the Orroli site.
Abbreviation: wi, Winter; sp, Spring; su, Summer; au, Autumn.

We evaluated the effect of the model uncertainties in our analysis, using a global multivariate approach based on a Monte Carlo simulation framework, generating 400 simulations through a simultaneous and independent variation of 4 parameters of the soil water model over a range of realistic values ($k_{sat} = 3 \times 10^{-7}$–$8 \times 10^{-7}$ m/s, $\theta_{lim,g} = 0.19 - 0.41$, $\theta_{lim,s} = 0.15 - 0.21$, $\theta_{lim,r} = 0.25 - 0.35$). The 5th and 95th percentiles of the ensemble of the $E_{t,fp}/LAI$ predictions are plotted in Figure 7b, confirming that the uncertainty of the $E_{t,fp}/LAI$ predictions is too small to affect the interpretation of the results – indeed, an increase of tree cover will likely lead to a persistently lower $E_{t,fp}/LAI$ during the summer.

Evaluating additional effects of the long-term trend of increasing dry conditions in spring (Figure 6), we compared the surface temperatures of trees and grass, D_z and ET during dry springs ($p < 0.8$ mm/d, and SPI < -1) and those observed during typical springs at the Orroli site during 2003–2017 (Figure 7c). While T_s was not significantly different for the tree clumps, it was significantly higher for grass in the dryer than typical springs (t-test, $p = 0.001$), showing a 7°C higher T_s, associated with higher D_z (32% on average), and lower ET (33%).

Finally, we evaluated the potential impact of land cover change strategies on historical soil water balance components (Figure 8), extending the soil water balance model estimation to the historical 1922–2017 period over the complete range of possible $F_{fp,t}$ (from 0 to 1). The long-term simulated trend of summer tree transpiration, which was not significant for the actual $F_{fp,t}$ case (=0.33), is significantly negative for increasing tree cover ($F_{fp,t} \geq 0.80$; Mann Kendall $\tau = -0.14$ for $F_{fp,t} = 1$), meaning that tree transpiration requirements could not have been met in such ecosystem as the climate progressively dried. Under the 100% tree cover scenario and increasingly dry climate, simulated ET trend become more negative in summer and autumn; this response to climate is significant only at $F_{fp,t} > 0.90$ (Figure 8c). In contrast, ET trend was positive in spring, significantly so at $F_{fp,t} > 0.80$ (Figure 8c). This trend was mostly impelled by the simulated positive trends of grass transpiration in spring, becoming significant at $F_{fp,t} > 0.50$ (Figure 8b). As expected, no trends of ET are simulated for grass dominated ecosystems where HR is limited (Figure 8c). In contrast, trends of drainage are negative for all seasons, but significantly so only in spring and winter and for all $F_{fp,t}$ scenarios (Figure 8e). The long-term trend of water uptake by tree roots from the rocky substratum was significantly positive for both spring and summer seasons under all land-cover scenarios (Figure 8d), driven by the progressively drying conditions in both seasons over the 1922–2017 period.

4. Discussion and Conclusion

In areas in which the vegetation remains active during a pronounced dry season, it must rely on water stored in the soil to sustain physiological activity and assure survival. However, the legacy of millennia of land-use over much of the mountainous terrain in the Mediterranean region, is shallow soils overlaying rocky strata. Yet some tree species remain active during the dry season, suggesting a substantial

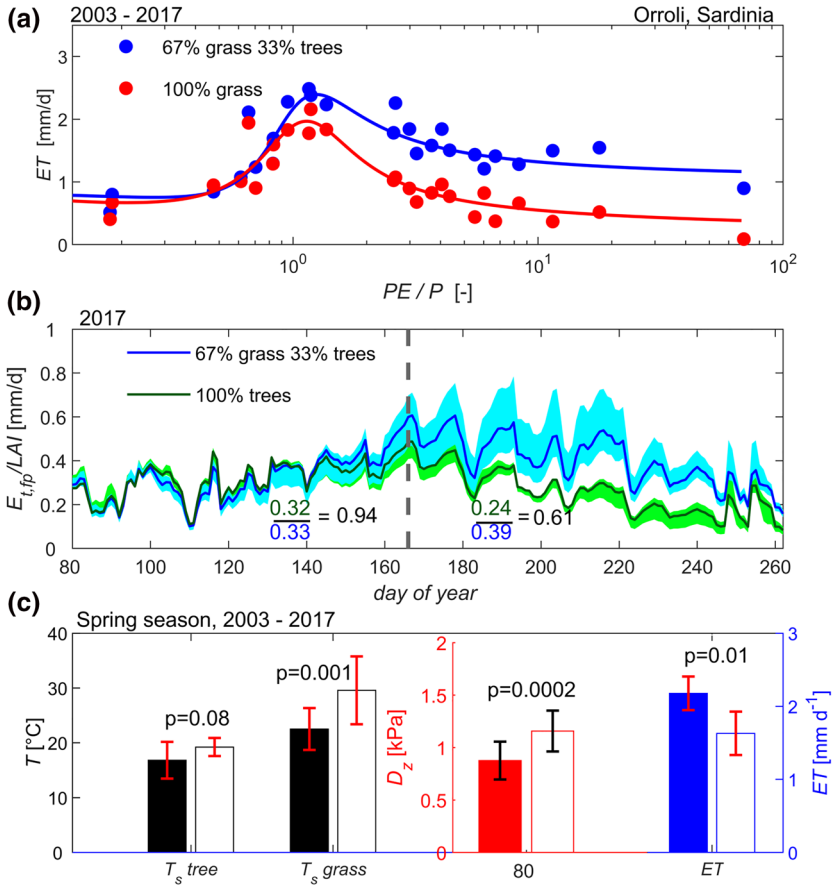

Figure 7. Comparison between the actual ecosystem and land cover change scenarios: (a) evapotranspiration (*ET*) versus dryness index (potential evaporation/precipitation, *PE*/*P*) for the actual ecosystem (67% pasture and 33% tree clumps), and for a hypothetical scenario of 100% pasture without the contribution of tree roots-induced hydraulic redistribution (HR). (b) Predicted tree transpiration at the footprint scale per unit of leaf area index ($E_{t,fp}/LAI$) for the actual ecosystem, and for a 100% tree cover scenario. Values in color represent the means for the season for each scenario, and the ratio represent the impact of eliminating HR from the prediction. The shaded areas around the mean bound the 5th and 95th percentiles of the ensemble of predictions generated with the Monte Carlo simulation framework. (c) Observed mean surface temperature (T_s) of tree and grass canopies, daytime, day-length normalized vapor pressure deficit (D_z), and evapotranspiration (*ET*) for typical ($n = 7$, filled bar) and dry ($n = 2$, unfilled bar) spring seasons (error bars are 1 standard deviations. *Note*: six incomplete spring time series and an unusually wet spring were excluded). Due to small sample size of dry springs, one sample t-test was used to assess the difference between the mean of the two dry years and the population of typical years.

supply of water from below the soil (Breshears et al., 2009; Schwinning, 2010). Here, we quantified the uptake of deep water by roots of wild olive trees penetrating into the fractured basalt below tree clumps, with canopy covering a third of the landscape, and into the surrounding, landscape-dominating seasonal vegetation.

Soil water budget, using precipitation (*P*), *ET*, and changes of soil moisture (ΔS; ~17 cm soil layer), suggests that deep water uptake by roots of wild olive trees, penetrating into the fractured basalt below tree clumps and the surrounding pasture, subsidizes grass transpiration in spring, likely through hydraulic redistribution. In summer, however, trees utilize all the deep water absorbed. Qualitative analysis of horizontal root distribution, soil moisture distribution, and water flow in roots over a summer drying cycle, supported hydraulic redistribution (HR) from the dry grass area and deeper below the tree clumps toward the shallow soil near the clumps. A 15-year data set shows that, as the seasonal drought-severity increases, the vertical water flux through the bottom of the thin soil layer transitions from drainage to uptake in support of *ET*. A 95-year precipitation and temperature data set shows that the dryness index of winter and spring, the two

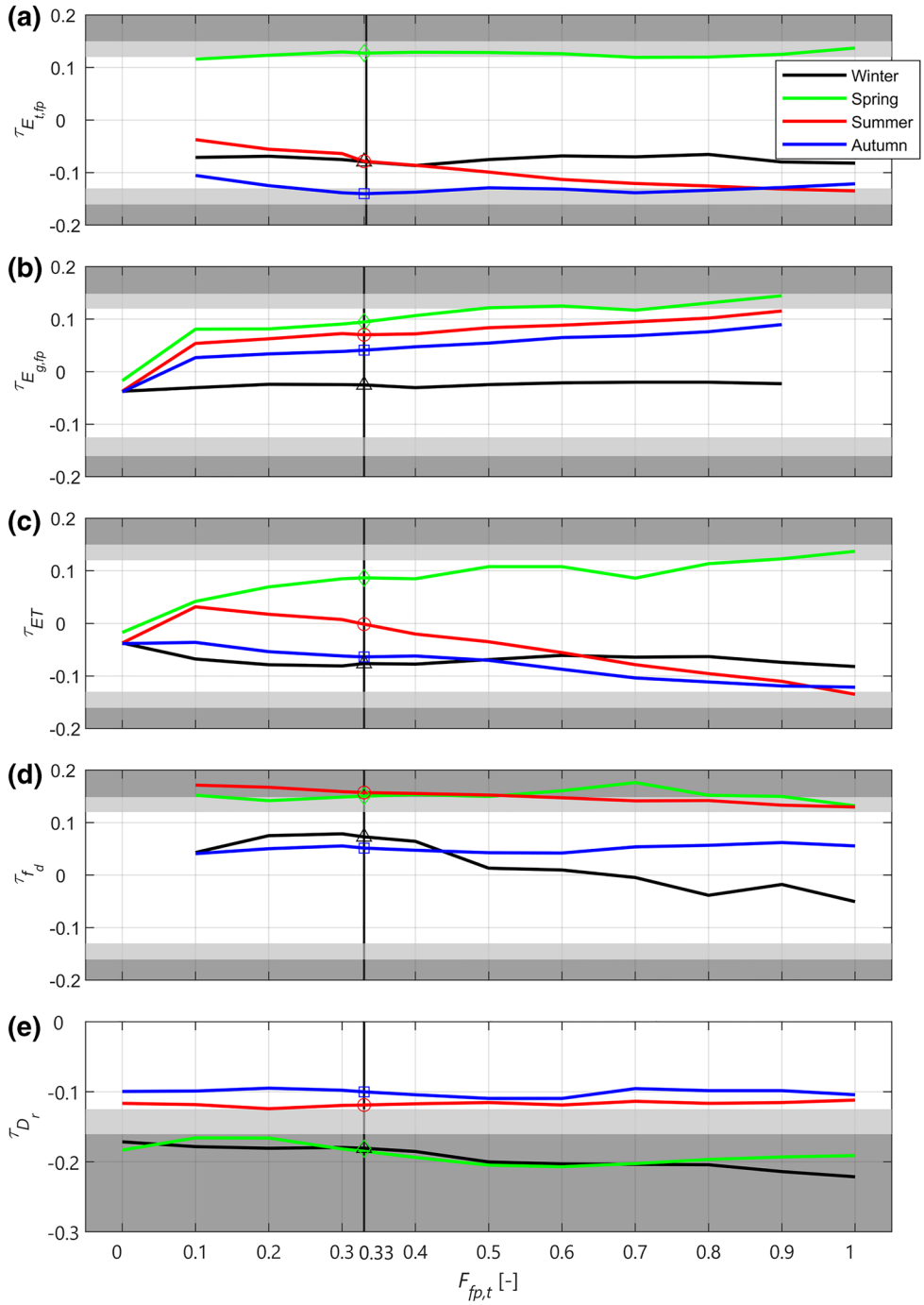

Figure 8. Seasonal Mann Kendall τ trends of tree transpiration at the footprint scale ($E_{t,fp}$), grass transpiration at the footprint scale ($E_{g,fp}$), evapotranspiration (ET), vertical flux through the bottom of the soil layer (f_d), and drainage (D_r) for the 1922–2017 period over the range of possible fraction of tree canopy cover ($F_{fp,t}$), The vertical black line shows the simulated results for the actual tree canopy cover at Orroli ($F_{fp,t} = 0.33$). The shaded areas represent the p value for the Mann Kendall τ trends ($p > 0.1$ for the white area, $p \leq 0.1$ and >0.05 for the light gray area, and $p \leq 0.05$ and ≥ 0.01).

key seasons for tree-grass ecosystems in water-limited Mediterranean ecosystems, is increasing, potentially affecting the equilibrium of this vegetation mosaic. We conclude with analyses of hypothetical scenarios in which the effect on *ET* is assessed for a landscape ranging in cover from only wild olive to only seasonal grass.

4.1. Water Balance and the Source of Evapotranspiration

The rock moisture uptake of tree species of semi-arid and arid environments has been recognized over a century ago (Cannon, 1911), yet we have found only few studies on the topic since Schwinning's (2010) proclamation (Barbeta et al., 2015; Estrada-Medina et al., 2013; Hasenmueller et al., 2017; Kukowski et al., 2013; Rempe & Dietrich, 2018). None of these studies assessed the importance of rock water uptake from under patches of adjacent, different cover-type vegetation in heterogeneous landscapes, and the importance of rock water to the function of these patches.

As do other tree species in the Mediterranean region, wild olive trees continue physiological activity and maintain transpiration during prolonged droughts when the moisture of the thin soil layer is at a stable minimum (Figure 1). This suggests that the trees function during the dry season by taking up water infiltrating during wet seasons into fractured rocks, perhaps stored in soil pockets (Estrada-Medina et al., 2013). Indeed, our soil water budget (Figures 2a and 2b) demonstrated that rock moisture uptake is essential for tree function in both spring and summer (consistent with **H1a**). Furthermore, our analysis also suggests that not only tree transpiration, but also transpiration and evaporation from grass-covered areas (and thus the energy and carbon balances) depend on deep water extraction by tree roots, especially during spring when the grass is active (contradicting **H2**; Figure 2d).

The water budget suggests that, in summer, trees use all the water their roots absorb below the soil (~0.8 mm/d), accounting for 100% of their transpiration. Although this may be achieved if trees could access ample rock moisture directly below the clumps, we later show otherwise. In contrast to summer, of the water taken up by tree roots from the fractured rock in spring (0.8–0.9 mm/d), the amount used by the trees was ~0.6 mm/d, with the rest (0.25 and 0.29 mm/d) contributing an average of 20% and 38% of the combined grass transpiration and bare-soil evaporation (in the wet and dry springs, respectively), likely through nightly hydraulic redistribution from the fractured rock to the soil (Domec et al., 2010; Neumann & Cardon, 2012; Yu & D'Odorico, 2015). This suggests that the grass, having its roots constrained to the shallow soil volume, must rely on rock moisture taken up and hydraulically redistributed into the overlaying soil by tree roots extending horizontally from clumps into the surrounding grass area (Figure 3).

Analysis of 15-year data suggests that, in this system, as the seasonal dryness index (potential evaporation/precipitation) increase over 1.04 (i.e., *PE* uses all of *P*, Figure 5), the vertical water flux through the bottom of the thin soil layer transitions from drainage, recharging deeper reservoirs and producing outflow, to uptake, supporting evapotranspiration. Based on the fit, the contribution of water taken up by tree roots from the rocky layer below the soil reaches a stable maximum of ~80% of *ET*, although the data suggests that during the most intense drought on record, >90% of summer *ET* is supported by this source. These estimates are consistent with another, where 91% of *ET* was met through uptake from rocky substrate in an area with annual precipitation of 550 mm (Schwinning, 2010). The analysis shows that the contribution to evapotranspiration of root water uptake from the rocky layer changes depending on seasonal precipitation and soil water storage. Generalizing our finding will require accounting for soil depth and characteristic, influencing water storage, and different types of vegetation and vegetation mosaic, affecting the rate and timing of water use.

4.2. Qualitative Assessment of Tree Water Uptake from the Surrounding Pasture

The water balance cannot be used to demonstrate the role horizontal tree roots play in hydraulic redistribution at the site. We acquired qualitative information that is, consistent with horizontal exchange of water between tree clumps and the surrounding grass-covered area, during a period in which the grass was inactive, and trees utilize most of the water they can obtain from the soil-rock system. In the very dry spring and summer of 2017, a period of summer rains increased soil moisture to a similar extent under the canopies near tree clumps and in the surrounding senesced grass area (Figure 4a). The directional sensors show that near the canopy flow was into trees (proximal) during daytime, and away from trees (distal) during nighttime, while the flow was proximal from the bare soil area both day and night (Figure 4b). Utilizing soil water near the clumps during the day requires recharge at night, with water obtained by deep roots in the rocky strata under the trees and the areas surrounding the clumps. After several days of incomplete recharge, the soil water potential near the canopy declined faster than in open areas. Later, as soil moisture reached similarly

low values under the canopy and in the open, hydraulic redistribution was constrained, obvious only in the small diurnal fluctuations of water potential, potentially reflecting decreased root-soil contact. Over the drying cycle, the contribution of moisture delivered by a root near the tree clump remained nearly constant relative to tree water use, but that of a root in the open declined as the soil dried, yet remain high even as the water potential gradient in the soil vanished (Figure 4c). This demonstrate that gradients in soil moisture has only limited influence on the horizontal flow of water in tree roots; this flow is likely influenced more by access to rock moisture under the canopy and under the surrounding grass-bare soil areas (consistent with hypothesis **H1b**).

4.3. Hypothetical Management and Climate Scenarios and Potential Consequences

The land cover management options require further assessment on the background of the long-term increasingly dry conditions in winter and spring (Figure 6).

4.3.1. Seasonal Grass Cover Only

A hypothetical landscape covered by pasture vegetation only, with no wild olive and access to deep water, would require 0.68–0.85 mm/d more than is available from precipitation and soil water storage (Figure 2), meaning it must have lower leaf area, or would have to complete its seasonal cycle earlier in spring. In such a landscape, carbon assimilation would be lower. Montaldo et al. (2013) estimated the spring (2005) water-use efficiency of a nearby grassland site (4 km from this study site) at 5 g C/kg H_20. A shortfall of $\sim$ 0.8 mm/d would thus amount to a reduced grass carbon assimilation of $\sim$ 4 g C m^{-2} d^{-1}, or $\sim$30% of its assimilation during the average spring day. In summer, such landscape would be in balance with the available water, but absent HR, *ET* would be 60% that of the existing wild olive-pasture mosaic. Based on Montaldo et al. (2013) this would increase surface temperature by 3°C and sensible heat flux by 10%. Higher surface temperature will likely decrease water-use efficiency further, especially during periods of Saharan Sirocco wind periods (Montaldo & Oren, 2016). Water taken up by tree roots from the rocky substratum was key to maintaining stomata open, allowing photosynthesis and, thus, survival and development of not only trees, but also of the seasonal vegetation in the pasture, likely through hydraulic redistribution. Having a third of the landscape surface covered by tree canopy, nearly doubled *ET* relative to the hypothetical treeless pasture, thus reducing skin temperature (Brutsaert, 1982; Seguin et al., 1994; Sun et al., 2016), especially during summer when $PE/P > 3.0$ (Figure 7a). The cost of lower skin temperature, however, is smaller water yield relative to landscapes covered with seasonal vegetation.

4.3.2. Evergreen Tree Cover Only

A hypothetical landscape covered only with wild olives of the same leaf area as in current clumps, would increase evapotranspiration, decreasing the average water yield by 58% in the falls of the 2003–2017 period. Despite using more water, trees will have to survive with $\sim$38% lower transpiration per unit leaf area in a dry summer (up to 50% at the end of the dry summer), potentially limiting survival and growth. The coupling between transpiration and CO_2 uptake for photosynthesis means that maintaining transpiration rate (per unit leaf area) is essential for proper function. A complete wild olive cover at current water use per unit leaf area is possible only if the entire ecosystem *LAI* is $\sim$2.5, as opposed to the $\sim$4.0 currently within tree clump areas; at the end of the summer *LAI* would have to be as low as 2.0 to maintain current gas exchange rates. Thus, a complete cover by forest will reduce water yield in this water-limited region, and eliminate the buffer offered to tree-clumps by the rock moisture under the current pasture area, a buffer that might decrease with winter precipitation. This may potentially force the ecosystem to undergo leaf area reduction in response to dry summers, mediated through partial tree mortality, thus increasing fuel and the likelihood of fires.

4.3.3. Seasonal-Evergreen Mosaic and Likely Future Changes

Long-term decreasing winter *P* and increasing spring *PE,* induce greater frequency of drought conditions during these seasons, reflected in a 60% increase of *PE*/*P* in 95 years and a doubling of severe droughts using SPI classification (Figure 6; Caloiero et al., 2019; Kannenberg et al., 2019; Montaldo & Sarigu, 2017; Philandras et al., 2011). The increasingly dry winter-spring conditions may have already enhanced the reliance of the grass on tree-root facilitated, hydraulically lifted rock moisture. This is reflected in the greater reliance on f_d in the spring of 2017 relative to a normal spring (Figure 2). It stands to reason that, with scenarios

predicting progressive decrease of winter precipitation and warmer springs over the next 70 years (Flato et al., 2013; Montaldo & Oren, 2018), the reliance of the grass patches on tree roots will increase, perhaps exceeding the capacity of tree clamps to provide sufficient water to maintain the current grass cover fraction. Indeed, in dry springs, *ET* decreased relative to typical springs, but only the grass surface temperature increased substantially (Figure 7c), suggesting increasing moisture stress. Thus, policies aimed at increasing water yield through tree removal may hasten the demise of the grass.

Even without intervention, the grass fraction likely become less active with increasing seasonal droughts. Will lower grass activity be a result of a shrinking grass cover and expansion of tree cover, or a shift to herbaceous species more adaptable to a shorter growing season? That wild olive has not produced shoots in the enclosure area (~120 m^2) surrounding the eddy-covariance tower since 2003, suggests that the proportional tree-grass cover represents an ecosystem in spatial equilibrium despite the increasing drought. This inference is strengthened by historical information on the spatial coverage of tree canopy at the site. For example, a 1954 aerial photography, despite its moderate resolution, showed wild-olive cover distribution at the Orroli site ($F_{fp,t} \sim 0.31$) remarkably similar to the most recent cover obtained 52 years later (~0.33; Figure S1). Thus, increasing drought conditions (Figures 6.9–6.12), accompanied with greater water uptake by trees in summer (Figure 6.19) and lesser recharge of rock water during winter (Figure 6.21), seem to have little effect on tree cover (Figure S1). One way in which the ecosystem may have acclimated to increasing drought (Figure 6), is through increased water consumption by trees in spring, increasing the water stress of seasonal vegetation, perhaps forcing changes in composition to dominance of species capable of completing their annual cycle earlier in spring, rather than a decrease in grass cover and increase in tree cover.

Indeed, over 35 years, the peak activity (reflected in NDVI) of the seasonal vegetation, composed mostly of grass species, progressively shifted two weeks earlier in spring, accelerating the completion of the annual life cycle. This may have been accomplished by a combination of acclimation of existing genotypes, a selection favoring genotypes completing their activity earlier in spring, or a shift in composition to such species. In addition to a retreat from traditional agro-silvopastoral activities, activities which kept tree cover low, increasing woodland cover in many area of the Mediterranean region (Chauchard et al., 2007; Falcucci et al., 2007; Poyatos et al., 2003; Puddu et al., 2012) may be facilitated by similar acclimation by the seasonal vegetation, freeing summer water to the wild olive. Alternatively, such acclimation by the seasonal component of these ecosystems may indicate that the entire ecosystem, including woody evergreen species experience water stress. If so, increased cover of the tree component may be constrained by low summer transpiration (and photosynthetic rate) per unit leaf area. We show (Figure 7b) that, in a landscape entirely covered by wild olive, gas exchange rate would be drastically curtailed, suggesting that such complete tree cover is unsustainable given the conditions at the site. We followed by evaluating, through simulations, how high the proportional tree cover at the Orroli site must be to cause a negative response of tree function to the historical changes in seasonal *P* and *PE* (shown in Figure 6).

We assessed the potential changes in certain components of the hydrologic budget, using the observed long-term climatic trends, imposed over the entire range of fractional vegetation cover (Figure 8). The outcome of this analysis permits determination of the fractional tree cover in which each hydrological component shows appreciable response to changing climate. Over historical climate change, the simulation shows minimal response of rock water recharge to climate trends during spring and summer when recharge was low, and of drainage in winter and spring, when the soil was moist and *ET* low. However, land cover does not affect the sensitivity of recharge and drainage to the trends in *P* and *PE* (Figures 8d and 8e). Similarly, spring and autumn tree transpiration show invariable sensitivity to the historical trends in *P* and *PE* over a wide range of tree cover, a range including the current 33% cover. Yet summer transpiration shows progressive increase in sensitivity, becoming significantly so at ~70% tree cover. This may suggest that, eliminating grazing from the site would allow wild olive cover to more than double. However, it is necessary to remember that, a small increase in the sensitivity of transpiration with tree cover would translate to a large increase in the sensitivity of transpiration per unit leaf area, because a greater tree cover means a proportionally higher tree *LAI*. This may explain why, despite nearly 20 years of grazing exclusion near the tower, wild olive cover did not increase.

Considering climate change-induced trends of decreasing water yield (Montaldo & Sarigu, 2017), increasing frequency of hot Sirocco winds (Montaldo & Oren, 2016), and the evidence of increasing ecosystem water

stress, a conversion to a homogeneous forest is unadvisable. The evidence for potentially large decrease in transpiration, and thus photosynthetic rate and tree survival, with increasing tree cover under changing climate, suggest that reforestation efforts may create stands with many dead individuals, increasing the risk of forest fire and catastrophic loss of carbon.

5. Conclusion

Vegetation growing in drier climates often display individual trees or tree clumps surrounded by seasonal vegetation. Increasing climatic drought, from long-term trends of decreasing precipitation in winter and increasing potential evapotranspiration in spring, is common in many dry regions. Where the balance among vegetation types in a mosaic depends on deep water to subsidize transpiration and related physiological activity, increasing drought may overwhelm the capacity for this subsidy, with consequences to land cover and biosphere-atmosphere exchanges. Here we show that, in patchy ecosystems, nighttime hydraulic lift of rock moisture by wild olive tree roots recharges the shallow soil, enough to support transpiration of grass and trees in spring, but rock moisture uptake from the entire area was just enough to meet the tree transpiration demand in summer. Thus, the seasonal vegetation relies on the evergreen tree component to maintain physiological performance in spring, while the evergreen trees rely on the inactivity of the seasonal component to maintain their own activity in the dry season. Patchy semi-arid and arid ecosystems likely represent a spatiotemporal balance of water supply, dynamically meeting the demand of two adjacent vegetation types of distinct seasonal phenology. The analysis suggests that this balance is sensitive to climate change. Thus, policies aimed at enhancing carbon sequestration by increasing tree cover, or water yield by increasing seasonal vegetation cover, may destabilize this equilibrium, with additional unintended consequences of decreasing tree survival or increasing surface temperature.

Data Availability Statement

Data of the Orroli site are made available at a central open-access repository (zenodo.org).

Acknowledgments
This study was supported by Ministry of Education, University and Research (MIUR) through the SWATCH European project of PRIMA MED program. Financial support for Ram Oren was provided by the Erkko Visiting Professor Programme of the Jane and Aatos Erkko 375th Anniversary Fund through the University of Helsinki. The authors acknowledge Giulio Vignoli, Gian Piero Deidda, Luigi Michele Noli, and Mario Sitzia, for ERT measurements, and Jean-Christophe Domec for instructions for the construction of root sensors. Finally, the authors thank the Meteoclimatic Department of ARPA Sardegna for providing meteorological data of the nearby stations (www.sar.sardegna.it).

References

Allen, M. F. (2009). Bidirectional water flows through the soil–fungal–plant mycorrhizal continuum. *New Phytologist*, *182*, 290–293.
Amirabadizadeh, M., Huang, Y. F., & Shui Lee, T. (2014). Recent trend in temperature and precipitation in the Langat River basin, Malaysia. *Advances in Meteorology*, *2015*, 1–16. https://doi.org/10.1155/2015/579437
Baldocchi, D. (2003). Assessing the eddy covariance technique for evaluating carbon dioxide exchange rates of ecosystems: Past, present and future. *Global Change Biology*, *9*, 1–14.
Baldocchi, D. D., Xu, L., & Kiang, N. (2004). How plant functional-type, weather, seasonal drought, and soil physical properties alter water and energy fluxes of an oak-grass savanna and an annual grassland. *Agricultural and Forest Meteorology*, *123*, 13–39.
Barbeta, A., Mejia-Chang, M., Ogaya, R., Voltas, J., Dawson, T. E., & Penuelas, J. (2015). The combined effects of a long-term experimental drought and an extreme drought on the use of plant-water sources in a Mediterranean forest. *Global Change Biology*, *21*(3), 1213–1225.
Batisani, N., & Yarnal, B. (2010). Rainfall variability and trends in semi-arid Botswana: Implications for climate change adaptation policy. *Applied Geography*. https://doi.org/10.1016/j.apgeog.2009.10.007
Bornyasz, M. A., Graham, R. C., & Allen, M. F. (2005). Ectomycorrhizae in a soil-weathered granitic bedrock regolith: Linking matrix resources to plants. *Geoderma*, *126*(1–2), 141–160.
Breshears, D. D. (2006). The grassland-forest continuum: Trends in ecosystem properties for woody plant mosaics? *Frontiers in Ecology and the Environment*, *4*(2), 96–104.
Breshears, D. D., Myers, O. B., & Barnes, F. J. (2009). Horizontal heterogeneity in the frequency of plant-available water with woodland intercanopy-canopy vegetation patch type rivals that occurring vertically by soil depth. *Ecohydrology*, *2*(4), 503–519.
Brunetti, M., Maugeri, M., Nanni, T., & Navarra, A. (2002). Droughts and extreme events in regional daily Italian precipitation series. *International Journal of Climatology*, *22*, 543–558. https://doi.org/10.1002/joc.751
Brutsaert, W. (1982). *Evaporation into the atmosphere: Theory, history, and applications* (p. 299). Kluwer Academic Publishers.
Caloiero, T., Coscarelli, R., Gaudio, R., & Leonardo, G. P. (2019). Precipitation trend and concentration in the Sardinia region. *Theoretical and Applied Climatology*, *137*, 297–307. https://doi.org/10.1007/s00704-018-2595-1
Cannon, A. W. (1911). *The root habits of desert plants* (p. 131). Carnege Institution of Washington.
Ceballos, A., Martinez-Fernandez, J., & Luengo-Ugidos, M. A. (2004). Analysis of rainfall trends and dry periods on a pluviometric gradient representative of Mediterranean climate in the Duero Basin, Spain. *Journal of Arid Environments*, *58*, 215–233. https://doi.org/10.1016/j.jaridenv.2003.07.002
Chauchard, S., Carcaillet, C., & Guibal, F. (2007). Patterns of land-use abandonment control tree-recruitment and forest dynamics in Mediterranean mountains. *Ecosystems*, *10*, 936–948. https://doi.org/10.1007/s10021-007-9065-4
Chow, V., Maidment, D., & Mays, L. (1988). *Applied hydrology*. New York: McGraw-Hill Book Company.

Clapp, R. B., & Hornberger, G. M. (1978). Empirical equations for some hydraulic properties. *Water Resources Research*, *14*, 601–604.
Connor, J. D. (2005). Adaptation of olive (Olea europaea L.) to water-limited environments. *Australian Journal of Agricultural Research*, *56*, 1181–1189.
Corona, R., Montaldo, N., & Albertson, J. D. (2018). On the role of NAO-driven interannual variability in rainfall seasonality on water resources and hydrologic design in a typical Mediterranean basin. *Journal of Hydrometeorology*, *19*(3), 485–498.
Detto, M., Montaldo, N., Albertson, J. D., Mancini, M., & Katul, G. (2006). Soil moisture and vegetation controls on evapotranspiration in a heterogeneous Mediterranean ecosystem on Sardinia, Italy. *Water Resources Research*, *42*(8), 16.
Dohn, J., Dembélé, F., Karembé, M., Moustakas, K., Amévor, A. K., & Hanan, N. P. (2013). Tree effects on grass growth in savannas: Competition, facilitation and the stress-gradient hypothesis. *Journal of Ecology*, *101*, 202–209.
Domec, J. C., King, J. S., Noormets, A., Treasure, E., Gavazzi, M. J., Sun, G., & McNulty, S. G. (2010). Hydraulic redistribution of soil water by roots affects whole-stand evapotranspiration and net ecosystem carbon exchange. *New Phytologist*, *187*(1), 171–183.
Eliades, M., Bruggeman, A., Lubczynski, M. W., Christou, A., Camera, C., & Djuma, H. (2018). The water balance components of Mediterranean pine trees on a steep mountain slope during two hydrologically contrasting years. *Journal of Hydrology*, *562*, 712–724. https://doi.org/10.1016/j.jhydrol.2018.05.048
Estrada-Medina, H., Graham, R. C., Allen, M. F., Jimenez-Osornio, J. J., & Robles-Casolco, S. (2013). The importance of limestone bedrock and dissolution karst features on tree root distribution in northern Yucatan, Mexico. *Plant and Soil*, *362*(1–2), 37–50.
Falcucci, A., Maiorano, L., & Boitani, L. (2007). Changes in land-use/land-cover patterns in Italy and their implications for biodiversity conservation. *Landscape Ecology*, *22*, 617–631. https://doi.org/10.1007/s10980-006-9056-4
Fernandez, J. E., Moreno, F., Giron, I. F., & Blazquez, O. M. (1997). Stomatal control of water use in olive tree leaves. *Plant and Soil*, *190*(2), 179–192.
Flato, G., Marotzke, J., Abiodun, B., Braconnot, P., Chou, S. C., Collins, W., et al. (2013). Evaluation of climate models. In T. F. Stocker, D. Qin, G.-K. Plattner, M. Tignor, S. K. Allen, J. Boschung, et al. (Eds.), *Climate change 2013: The physical science basis. Contribution of Working Group I to the Fifth Assessment Report of the Intergovernmental Panel on Climate Change*. Cambridge, United Kingdom and New York, NY, USA: Cambridge University Press.
Franks, S. W., Beven, K. J., Quinn, P. F., & Wright, I. R. (1997). On the sensitivity of soil vegetation atmosphere transfer (SVAT) schemes: Equifinality and the problem of robust calibration. *Agricultural and Forest Meteorology*, *86*, 63–75.
Garcia-Ruiz, J. M., López-Moreno, J. J., Vicente-Serrano, S. M., & Beguería, S. (2011). Mediterranean water resources in a global change scenario. *Earth-Science Reviews*, *105*(3–4), 121–122. https://doi.org/10.1016/j.earscirev.2011.01.006
Gentry, A. H., & Lopez-Parodi, J. (1980). Deforestation and increased flooding of the upper Amazon. *Science*, 1354–1356. https://doi.org/10.1126/science.210.4476.1354
Graham C. R., Rossi M. R. & Hubbert R. (2010). Rock to regolith conversion: Producing hospitable substrates for terrestrial ecosystems. *GSA Today*, *20*(2).
Graham, C. R., Schoeneberger, J. P., Anderson, A. M., Stemberg, D. P., & Tice, R. K. (1997). Morphology, porosity, and hydraulic conductivity of weathered granitic bedrock and overlying soils. *Soil Science Society of America Journal*, *61*, 516–522.
Granier, A. (1987). Evaluation of transpiration in a Douglas-fir stand by means of sap flow measurements. *Tree Physiology*, *3*, 309–320.
Griebel, A., Bennett, L. T., Metzen, D., Cleverly, J., Burba, G., & Arndt, S. K. (2016). Effects of inhomogeneities within the flux footprint on the interpretation of seasonal, annual, and interannual ecosystem carbon exchange. *Agricultural and Forest Meteorology*, *221*, 50–60.
Guttman, N. B. (1998). Comparing the palmer drought index and the standardized precipitation index. *Journal of the American Water Resources Association*, *34*(1).
Guzha, A. C., Rufino, M. C., Okoth, S., Jacobs, S., & Nóbrega, R. L. B. (2018). Impacts of land use and land cover change on surface runoff, discharge and low flows: Evidence from East Africa. *Journal of Hydrology: Regional Studies*, *15*, 49–67. https://doi.org/10.1016/j.ejrh.2017.11.005
Hasenmueller, E. A., Gu, X., Weitzman, J. N., Adams, T. S., Stinchcomb, G. E., Eissenstat, D. M., et al. (2017). Weathering of rock to regolith: The activity of deep roots in bedrock fractures. *Geoderma*, *300*, 11–31.
Hensel, D. R., & Hirsch, R. H. (2002). *Statistical method in water resources* USGS science for a changing world. Chapter A3.
Hirsch, R. H., Slack, J. R., & Smith, A. (1982). Techniques of trend analysis for monthly water quality data. *Water Resources Research*, *18*(1), 107–121. https://doi.org/10.1029/WR018i001p00107
House, J. I., Archer, S., Breshears, D. D., & Scholes, R. J. (2003). Conundrums in mixed woody-herbaceous plant systems. *Journal of Biogeography*, *30*(11), 1763–1777.
Hu, Y., Maskey, S., & Uhlenbrook, S. (2012). Trends in temperature and rainfall extremes in the Yellow River source region, China. *Climatic Change*, *110*, 403–429. https://doi.org/10.1007/s10584-011-0056-2
Huang, J., Ji, M., Xie, Y., Wang, S., He, Y., & Ran, J. (2016). Global semi-arid climate change over last 60 years. *Climate Dynamics*, *46*(3–4), 1131–1150.
Hubbert, R. K., Graham, C. R., & Anderson, A. M. (2001). Soil and weathered bedrock: Components of a Jeffrey pine plantation substrate. *Soil Science Society of America Journal*, *65*, 1255–1262.
Imukova K., Ingwersen J., Hevart M., & Streck T. (2016). Energy balance closure on a winter wheat stand: Comparing the eddy covariance technique with the soil water balance method. *Biogeosciences*, *13*, 63–75. https://doi.org/10.5194/bg-13-63-2016
Kannenberg, S. A., Novick, K. A., Alexander, M. R., Maxwell, J. T., Moore, D. J., Phillips, R. P., & Anderegg, W. R. (2019). Linking drought legacy effects across scales: From leaves to tree rings to ecosystems. *Global Change Biology*, *25*, 2978–2992. https://doi.org/10.1111/gcb.14710
Kendall, M. G. (1938). A new measure of rank correlation. *Biometric Trust*, *30*, 81–93. https://doi.org/10.2307/2332226
Kukowski, K. R., Schwinning, S., & Schwartz, B. F. (2013). Hydraulic responses to extreme drought conditions in three co-dominant tree species in shallow soil over bedrock. *Oecologia*, *171*(4), 819–830.
Kurc, S. A., & Small, E. E. (2004). Dynamics of evapotranspiration in semiarid grassland and shrubland ecosystems during the summer monsoon season, central New Mexico. *Water Resources Research*, *40*, W09305. https://doi.org/10.1029/2004WR003068
Lewis, D. C., & Burgy, R. H. (1964). The relationship between oak tree roots and groundwater in fractured rock as determined by tritium tracing. *Journal of Geophysical Research*, *69*(12), 2579–2588.
Lindner, M., Fitzgerald, J. B., Zimmermann, N. E., Reyer, C., Delzon, S., vander Maaten, E., et al. (2014). Climate change and European forests: What do we know, what are the uncertainties, and what are the implications for forest management? *Journal of Environmental Management*, *146*, 69–83. https://doi.org/10.1016/j.jenvman.2014.07.030

Liski, J., Korotkov, A. V., Prins, C. F. L., et al. (2003). Increased carbon sink in temperate and boreal forests. *Climatic Change, 61*, 89–99. https://doi.org/10.1023/A:1026365005696

Livada, I., & Assimakopoulos, V. (2007). Spatial and temporal analysis of drought in Greece using the Standardized Precipitation Index (SPI). *Theoretical and Applied Climatology*, *89*, 143–153. https://doi.org/10.1007/s00704-005-0227-z

Lo Gullo, M. A., & Salleo, S. (1988). Different strategies of drought resistance in three Mediterranean sclerophyllous trees growing in the same environmental conditions. *New Phytologist*, *108*, 267–276.

Ludwig, F., Dawson, T. E., Prins, H. H. T., Berendse, F., & de Kroon, H. (2004). Below-ground competition between trees and grasses may overwhelm the facilitative effects of hydraulic lift. *Ecology Letters*, *7*(8), 623–631.

Lumaret, R., & Ouazzani, N. (2001). Brief communications. *Nature*, *413*.

Maselli, F., Chiesi, M., & Bindi, M. (2004). Multi-year simulation of Mediterranean forest transpiration by the integration of NOAA-AVHRR and ancillary data. *International Journal of Remote Sensing*, *25*(19), 3929–3941.

McCole, A. A., & Stern, L. A. (2007). Seasonal water use patterns of Juniperus ashei on the Edwards Plateau, Texas, based on stable isotopes in water. *Journal of Hydrology*, *342*(3–4), 238–248.

Mishra, A. K., & Singh, V. P. (2009). Analysis of drought severity-area-frequency curves using a general circulation model and scenario uncertainty. *Atmosphere*, *114*, D06120. https://doi.org/10.1029/2008JD010986

Mohammad, A. G., & Adam, M. A. (2010). The impact of vegetative cover type on runoff and soil erosion under different land uses. *Catena*, *81*(2), 97–103. https://doi.org/10.1016/j.catena.2010.01.008

Mohsin, T., & Gough, W. A. (2010). Trend analysis of long-term temperature time series in the Greater Toronto Area (GTA). *Theoretical and Applied Climatology*, *101*, 311–327. https://doi.org/10.1007/s00704-009-0214-x

Montaldo, N., Albertson, J. D., & Mancini, M. (2008). Vegetation dynamics and soil water balance in a water-limited Mediterranean ecosystem on Sardinia, Italy. *Hydrology and Earth System Sciences*, *12*, 1257–1271.

Montaldo, N., Corona, R., & Albertson, J. D. (2013). On the separate effects of soil and land cover on Mediterranean ecohydrology: Two contrasting case studies in Sardinia, Italy. *Water Resources Research*, *49*, 1123–1136.

Montaldo, N., Curreli, M., Corona, R., & Oren, R. (2020). Fixed and variable components of evapotranspiration in a Mediterranean wild-olive-grass landscape mosaic. *Agricultural and Forest Meteorology*, *280*, 107769. https://doi.org/10.1016/j.agrformet.2019.107769

Montaldo, N., & Oren, R. (2016). The way the wind blows matters to ecosystem water use efficiency. *Agricultural and Forest Meteorology*, *217*, 1–9.

Montaldo, N., & Oren, R. (2018). Changing seasonal rainfall distribution with climate directs contrasting impacts at evapotranspiration and water yield in the western Mediterranean region. *Earth's Future*. https://doi.org/10.1029/2018EF000843

Montaldo, N., & Sarigu, A. (2017). Potential links between the North Atlantic Oscillation and decreasing precipitation and runoff on a Mediterranean area. *Journal of Hydrology*, *553*, 419–437.

Moore, G. W., & Heilman, J. L. (2011). Proposed principles governing how vegetation changes affect transpiration. *Ecohydrology*, *4*(3), 351–358.

Muchingami, I., Hlatywayo, D. J., Nel, J. M., & Chuma, C. (2012). Electrical resistivity survey for groundwater investigations and shallow subsurface evaluation of the basaltic-greenstone formation of the urban Bulawayo aquifer. *Physics and Chemistry of the Earth*, *50–52*, 44–51.

Neumann, R. B., & Cardon, Z. G. (2012). The magnitude of hydraulic redistribution by plant roots: A review and synthesis of empirical and modeling studies. *New Phytologist*, *194*(2), 337–352.

Nie, Y. P., Chen, H. S., Ding, Y. L., Yang, J., Wang, K. L. (2017). Comparison of rooting strategies to explore rock fractures for shallow soil-adapted tree species with contrasting aboveground growth rates: A greenhouse microcosm experiment, *Frontiers of Plant Science*, *8*, 1651–1661. https://doi.org/10.3389/fpls.2017.01651

Nijland, W., van der Meijde, M., Addink, E. A., & deJong, S. M. (2010). Detection of soil moisture and vegetation water abstraction in a Mediterranean natural area using electrical resistivity tomography. *Catena*, *81*(3), 209–216.

Noilhan, J., & Planton, S. (1989). A simple parameterization of land surface processes for meteorological models. *Monthly Weather Review*, *117*, 536–549.

Oishi, A. C., Oren, R., & Stoy, P. C. (2008). Estimating components of forest evapotranspiration: A footprint approach for scaling sap flux measurements. *Agricultural and Forest Meteorology*, *148*(11), 1719–1732.

Oren, R., Phillips, N., Katul, G., Ewers, B. E., & Pataki, D. E. (1998). Scaling xylem sap flux and soil water balance and calculating variance: A method for partitioning water flux in forests. *Annales des Sciences Forestieres*, *55*(1–2), 191–216.

Oren, R., Zimmermann, R., & Terborgh, J. (1996). Transpiration in upper Amazonia floodplain and upland forests in response to drought breaking rains. *Ecology*, *77*, 968–973.

Ovando, P., Beguería, S., & Campos, P. (2019). Carbon sequestration or water yield? The effect of payments for ecosystem services on forest management decisions in Mediterranean forests. *Water Resources and Economics*, *28*, 100119.

Parlange, M. B., Albertson, J. D., Eichinger, W. E., Cahill, A. T., & Jackson, T. J. (1999). Evaporation: Use of fast response turbulence sensors, Raman lidar and passive microwave remote sensing. In M. B. (Ed.), *Vadose zone hydrology: Cutting across disciplines*.

Philandras, C. M., Nastos, P. T., Kapsomenakis, J., Douvis, K. C., Tselioudis, G., & Zerefos, C. S. (2011). Long term precipitation trends and variability within the Mediterranean region. *Natural Hazards and Earth System Sciences*, *11*, 3235–3250. https://doi.org/10.5194/nhess-11-3235-2011

Ponce, V. M. (1989). *Engineering hydrology* (p. 640). NJ: Prentice Hall.

Poyatos, R., Latron, J., & Pilar, L. (2003). Land use and land cover change after agricultural abandonment. *Mountain Research and Development*, *23*(4), 362–368.

Puddu, G., Falcucci, A., & Maiorano, L. (2012). Forest changes over a century in Sardinia: Implications for conservation in a Mediterranean hotspot. *Agroforest System*, *85*, 319–330.

Pungetti, G. (1985). Anthropological approach to agricultural landscape history in Sardinia. *Landscape and Urban Planning*, *31*, 47–56.

Quijano, J. C., Kumar, P., Drewry, D. T., Goldstein, A., & Misson, L. (2012). Competitive and mutualistic dependencies in multispecies vegetation dynamics enabled by hydraulic redistribution. *Water Resources Research*, *48*, W05518. https://doi.org/10.1029/2011WR011416

Raz-Yaseef, N., Rotenberg, E., & Yakir, D. (2010). Effects of spatial variations in soil evaporation caused by tree shading on water flux partitioning in a semi-arid pine forest. *Agricultural and Forest Meteorology*, *150*(3), 454–462.

Reicherta, J. M., Rodrigues, M. F., Peláez, J. J. Z., Lanza, R., Minella, J. P. G., Arnold, J. G., & Cavalcante, R. B. L. (2017). Water balance in paired watersheds with eucalyptus and degraded grassland in Pampa biome. *Agricultural and Forest Meteorology*, *237–238*, 282–295. https://doi.org/10.1016/j.agrformet.2017.02.014

Rempe, D. M., & Dietrich, W. E. (2018). Direct observations of rock moisture, a hidden component of the hydrologic cycle. *Proceedings of the National Academy of Sciences of the United States of America*, *115*(11), 2664–2669.
Reynolds, J., Kemp, P., & Tenhunen, J. (2000). Effects of long-term rainfall variability on evapotranspiration and soil water distribution in the Chihuan desert: A modeling analysis. *Plant Ecology*, *150*, 145–159.
Rodriguez-Iturbe, I. (2000). Ecohydrology: A hydrologic perspective of climate-soil-vegetation dynamics. *Water Resources Research*, *36*(1), 3–9.
Rodriguez-Robles, U., Arredondo, T., Huber-Sannwald, E., Ramos-Leal, J. A., & Yepez, E. A. (2017). Technical note: Application of geophysical tools for tree root studies in forest ecosystems in complex soils. *Biogeosciences*, *14*(23), 5343–5357.
Rose, K. L., Graham, R. C., & Parker, D. R. (2003). Water source utilization by Pinus jeffreyi and Arctostaphylos patula on thin soils over bedrock. *Oecologia*, *134*(1), 46–54.
Sankaran, M., Hanan, N. P., Scholes, R. J., Ratnam, J., Augustine, D. J., Cade, B. S., et al. (2005). Determinants of woody cover in African savannas. *Nature*, *438*(7069), 846–849.
Scholes, R. J., & Archer, S. R. (1997). Tree-grass interactions in savannas. *Annual Review of Ecology, Evolution, and Systematics*, *28*, 517–544.
Schwinning, S. (2008). The water relations of two evergreen tree species in a karst savanna. *Oecologia*, *158*, 373–383. https://doi.org/10.1007/s00442-008-1147-2
Schwinning, S. (2010). Ecohydrology Bearings - Invited Commentary: The ecohydrology of roots in rocks. *Ecohydrology*, *3*, 238–245.
Seguin, B., Courault, D., & Guerif, M. (1994). Surface-temperature and evapotranspiration: Application of local scale methods to regional scales using satellite data. *Remote Sensing of Environment*, *49*(3), 287–295.
Sen, P. K. (1968). Estimates of the regression coefficient based on Kendall's tau. *Journal of the American Statistical Association*, *63*, 1379–1389. https://doi.org/10.2307/2285891
Sneyers, S. (1990). *On the statistical analysis of series of observations* (p. 192). Technical Note No. 143. World Meteorological Organization. ISBN: 19912451385.
Soil Conservation Service (1972). *National engineering handbook, hydrology, section 4*. Washington, DC: US Department of Agriculture.
Soil Conservation Service (1986). *National engineering handbook, hydrology, section 4*. Washington, DC: US Department of Agriculture.
Stephens, S. L., Millar, C. I., & Collins, B. M. (2010). Operational approaches to managing forests of the future in Mediterranean regions within a context of changing climates. *Environmental Research Letters*, *5*, 024003. https://doi.org/10.1088/1748-9326/5/2/024003
Sternberg, P. D., Anderson, M. A., Graham, R. C., Beyers, J. L., & Tice, K. R. (1996). Root distribution and seasonal water status in weathered granitic bedrock under chaparral. *Geoderma*, *72*(1–2), 89–98.
Sun, Z. G., Wang, Q. X., Batkhishig, O., & Ouyang, Z. (2016). Relationship between evapotranspiration and land surface temperature under energy- and water-limited conditions in dry and cold climates. *Advances in Meteorology*, 1–9.
Swain, D. L., Horton, D. E., Singh, D., & Diffenbaugh, N. S. (2016). Trends in atmospheric patterns conducive to seasonal precipitation and temperature extremes in California. *Science Advances*, *2*, e1501344.
Tabari, H., Abghari, H., & Talaee, P. H. (2012). Temporal trends and spatial characteristics of drought and rainfall in arid and semiarid regions of Iran. *Hydrological Processes*, *26*, 3351–3361.
Terral, J. F., Badal, E., Heinz, C., Roiron, P., Thiebault, S., & Figueiral, I. (2004). A hydraulic conductivity model points to post-Neogene survival of the Mediterranean olive. *Ecology*, *85*(11), 3158–3165.
Theil, H. (1950). A rank-invariant method of linear and polynomial regression analysis. *Proceedings of the Koninklijke Nederlandse Akademie Wetenschappen*, *53*, 386–392, 512–525, 1397–1412.
Thornthwaite, C. W. (1948). An approach toward a rational classification of climate. *Geographical Review*, *38*, 55–94.
Travelletti, J., Sailhac, P., Malet, J. P., Grandjean, G., & Ponton, J. (2012). Hydrological response of weathered clay-shale slopes: Water infiltration monitoring with time-lapse electrical resistivity tomography. *Hydrological Processes*, *26*(14), 2106–2119.
Vilà-Cabrera A., Coll, L., Martínez-Vilalta, J., & Retana, J. (2018). Forest management for adaptation to climate change in the Mediterranean basin: A synthesis of evidence. *Forest Ecology and Management*, *407*, 16–22. https://doi.org/10.1016/j.foreco.2017.10.021
Villegas, J. C., Espeleta, J. E., Morrison, C. T., Breshears, D. D., & Huxman, T. E. (2014). Factoring in canopy cover heterogeneity on evapotranspiration partitioning: Beyond big-leaf surface homogeneity assumptions. *Journal of Soil and Water Conservation*, *69*(3), 78A–83A.
Webb E. K., Pearman G. I., Leuning R. (1980). Correction of flux measurements for density effects due to heat and water vapour transfer. *Quaterly Journal of Royal Meteorological Society*, *106*:85–100. https://doi.org/10.1002/qj.49710644707
Wilson, T. G., Cortis, C., Montaldo, N., & Albertson, J. D. (2014). Development and testing of a large, transportable rainfall simulator for plot-scale runoff and parameter estimation. *Hydrology and Earth System Sciences*, *18*, 4169–4183.
Witty, J. H., Graham, R. C., Hubbert, K. R., Doolittle, J. A., & Wald, J. A. (2003). Contributions of water supply from the weathered bedrock zone to forest soil quality. *Geoderma*, *114*(3–4), 389–400.
Yan, Y., Dai, Q., Jin, L., & Wang, X. (2019). Geometric morphology and soil properties of shallow karst fissures in an area of karst rocky desertification in SW China. *Catena*, *107*, 48–58.
Yu, K., & D'Odorico, P. (2015). Hydraulic lift as a determinant of tree–grass coexistence on savannas. *New Phytologist*, *207*, 1038–1051. https://doi.org/10.1111/nph.13431
Zhang, L., Dawes, W. R., & Walker, G. R. (2001). Response of mean annual evapotranspiration to vegetation changes at catchment scale. *Water Resources Research*, *37*(3), 701–708.
Zwieniecki, M. A., & Newton, M. (1995). Roots growing in rock fissures: Their morphological adaptation. *Plant and Soil*, *172*(2), 181–187.